

Volatile electricity markets and battery storage: A model-based approach for optimal control

Wilfried Kenmoe Nzali^{1,2}, Christian Bayer¹, Dörte Kreher², Manuel Landstorfer¹

submitted: December 18, 2025

¹ Weierstrass Institute
Anton-Wilhelm-Amo-Str. 39
10117 Berlin
Germany
E-Mail: kenmoe@wias-berlin.de
christian.bayer@wias-berlin.de
manuel.landstorfer@wias-berlin.de

² Humboldt-Universität zu Berlin
Unter den Linden 6
10099 Berlin
Germany
E-Mail: wilfried.kenmoe.nzali@student.hu-berlin.de
doerte.kreher@hu-berlin.de

No. 3248
Berlin 2025



2020 *Mathematics Subject Classification.* 93E20, 91B74, 34A12, 49L20, 90C39.

Key words and phrases. Stationary battery storage device, electricity spot price, stochastic optimal control, dynamic programming, least squares Monte-Carlo, electricity consumption cost, amortization time.

All authors gratefully acknowledge funding by the Deutsche Forschungsgemeinschaft (DFG, German Research Foundation) under Germany's Excellence Strategy – The Berlin Mathematics Research Center MATH+ (EXC-2046/1, project ID: 390685689) via the project AA4-9.

Edited by
Weierstraß-Institut für Angewandte Analysis und Stochastik (WIAS)
Leibniz-Institut im Forschungsverbund Berlin e. V.
Anton-Wilhelm-Amo-Straße 39
10117 Berlin
Germany

Fax: +49 30 20372-303
E-Mail: preprint@wias-berlin.de
World Wide Web: <http://www.wias-berlin.de/>

Volatile electricity markets and battery storage: A model-based approach for optimal control

Wilfried Kenmoe Nzali, Christian Bayer, Dörte Kreher, Manuel Landstorfer

Abstract

Grid connected energy storage systems provide a strategic advantage by exploiting electricity market price fluctuations, thereby significantly reducing energy consumption costs. This paper presents a general framework for minimizing electricity consumption costs by formulating the problem as a stochastic optimal control problem for a stationary battery storage device (SBSD). We propose a realistic model for electricity spot prices calibrated with real data, alongside a detailed model of battery dynamics with practical parameters. The control problem is solved in a discrete time setting by combining dynamic programming with the least squares Monte Carlo method, allowing us to approximate the value function and the optimal policy under both state of charge and voltage constraints. Using the derived optimal policy, we estimate the lower bound of electricity consumption costs across multiple price trajectories. The results demonstrate that the SBSBD can substantially reduce consumption costs, with savings increasing with battery duration. After one year, a battery with 12 hours duration achieves approximately 11% cost reduction, while 24 hours battery achieves 21%, compared to a scenario without storage. Finally, we estimate the amortization time (the period required for cumulative savings to offset the initial investment). After 6.7 years for the 12 hours battery and 9.9 years for the 24 hours battery, the amortization time is reached.

1 Introduction

1.1 Motivation

The global shift toward sustainable energy has accelerated the transition from traditional polluting sources such as fossil fuels (coal, oil, and natural gas) and nuclear energy toward cleaner alternatives like solar, wind, and hydropower. By 2050, renewable energy sources have the potential to supply as much as 85% of the global electricity demand [ETI25]. Despite the fact that these renewable sources offer environmental and economic benefits, they also introduce significant challenges, particularly in terms of energy storage. In particular, electricity generated from renewable sources is inherently subject to seasonal variability such as fluctuations in wind intensity or solar intensity making efficient energy storage systems indispensable for ensuring continuous supply and maintaining grid stability. Battery storage systems have emerged as a crucial solution to address these challenges. By enabling electricity to be stored during periods of low demand or low market prices and discharged during peak demand or high prices, they offer a solution to stabilize the grid and optimize energy usage [CWCY25, EGASNH25]. This dual capability not only supports the integration of renewables but also opens up opportunities for cost efficient energy management. In this study, we investigate the strategic use of a stationary battery storage device within the context of electricity consumption in uncertain electricity markets. In reality, electricity spot markets exhibit complex price fluctuations driven by supply demand imbalances, regulatory factors, and external shocks. Consumers equipped with battery systems can leverage these price dynamics to minimize their overall electricity consumption costs by charging the battery when prices are low and discharging when prices are high [SDD24].

1.2 Related works and own contribution

In recent years, the optimal control of a battery storage device has gained increased attention in the engineering and applied mathematics community. Particularly studying the problem within the framework of stochastic control theory allows for the modelling of uncertainties inherent in electricity prices and consumption patterns, providing a robust foundation for decision-making under risk. Recent research has explored various methodologies for solving such control problems, including dynamic programming, reinforcement learning, and simulation-based techniques [MZC⁺20]. These methods aim to derive optimal policies that balance consumption cost minimization with operational constraints, such as battery capacity, degradation, and market regulations. In [NNN25], the challenge of operating a Battery Energy Storage System (BESS) under uncertainty from renewable sources like PV and wind in micro grids is addressed, based on model predictive control techniques using a coyote algorithm. Using deep reinforcement learning, [CMBP⁺25] builds a framework for optimizing

the participation of collocated renewable energy sources (RES) and BESS across multiple electricity markets. In [CT18], a novel scheduling strategy for micro grids operating in volatile electricity markets is developed, integrating financial portfolio theory to maximize economic returns while maintaining operational feasibility. In [VM25] a detailed economic assessment of BESS operating in both day-ahead and intraday electricity markets is studied, with a unique focus on how battery bids influence market prices. Furthermore, [PPW⁺20] addresses the challenge of fast-charging Li-ion batteries without damage by proposing a model-free reinforcement learning approach to overcome limitations of traditional model-based optimal control, such as parameter uncertainty and aging effects. The strategy demonstrates online adaptability to environmental variations and state reduction while ensuring safety constraints. More recently, [SDD24] studies the optimal control of battery storage in energy markets, especially the German electricity market. They use a VAR model to model prices and analyse battery profitability as a function of price volatility in 2020 and 2023. They show that low price volatility in 2020 does not allow profitable operation, while increased instability in 2023 offers better profit opportunities.

By extending the existing literature, this paper addresses the unresolved challenge of controlling stationary battery storage under stochastic electricity pricing while accounting for internal battery state constraints (not only state of charge but also voltage constraint). Our main contribution is the introduction of a tractable stochastic optimal control framework that delivers accurate approximations of optimal policies in energy systems. This framework enables cost efficient battery usage even in volatile electricity markets, thereby bridging the gap between theoretical modelling and practical applications relevant to both academia and industry. The novelty of our approach lies in combining a realistic stochastic electricity price model with a physically detailed battery representation with voltage dynamic incorporated, which together yield a highly non-linear system of stochastic differential equations. To address the resulting complexity, we develop efficient numerical methods based on the dynamic programming equation and the least squares Monte Carlo (LSMC) method. This methodological innovation offers a scalable and implementable solution to a problem that has, until now, been treated in a largely simplified manner in prior work.

1.3 Organization of the paper

The rest of this paper is organized as follows. In Section 2 we describe the electricity spot price model, the battery model, and the consumer's power demand utilized in the study. In Section 3 we present the optimal control problem in continuous time. In Section 4 we discuss methodologies for solving the optimal control problem in discrete time, employing dynamic programming and the LSMC method. In Section 5 we analyze the simulation results of the proposed dynamics. In Section 6 we explore the amortization time. Finally Section 7 concludes by summarizing the key findings of the study.

2 Modelling Section

2.1 Electricity spot price model

The pricing of electricity on the energy market is linked to the dynamics of both, supply and demand, resulting in a stochastic behaviour. However, we observe various seasonal patterns, including daily, weekly, and monthly cycles, in the dynamics of electricity prices. Generally, deterministic functions are employed to capture these variations. Moreover, given the unpredictable nature of electricity markets, it is imperative to incorporate stochastic processes that effectively replicate the inherent volatility observed in electricity prices. Let us denote by S a state vector of dimension $d_s \in \mathbb{N}$. In our setting, we assume that the only state variable is the electricity spot price and hence S is one-dimensional, i.e. $d_s = 1$.

We define the model for the electricity spot price $S = (S(t))_{t \geq 0}$ by

$$S(t) = \Lambda(t) + P(t), \quad t \geq 0, \quad (1)$$

where Λ is the deterministic seasonality component and P is a stochastic process. Throughout this work, time t is measured in hour.

Deterministic seasonality Λ

Λ is modelled as a combination of multiple functions, including a linear trend and a cosine component to capture the yearly variation of electricity prices, an approach widely used in the literature, cf. e.g. [Ver16]. To account for weekly and hourly variations, we additionally include 24×7 indicator functions $\chi_{d,h}$ (dummy variables), which are binary indicators effectively

capturing discrete changes associated with specific temporal units. $\chi_{d,h}$ can be written as follows

$$\chi_{d,h}(t) = \begin{cases} 1, & \text{if at time } t \text{ the day of the week is } d \text{ and the hour is } h, \\ 0, & \text{otherwise.} \end{cases} \quad (2)$$

Here, $d \in \{0, 1, 2, 3, 4, 5, 6\}$ represents the day of the week (i.e., 0 = Monday, \dots , 6 = Sunday) and $h \in \{0, 1, 2, \dots, 23\}$ represents the hour of the day. This choice is motivated by the findings of [KWZ23, KPS19], who show that using indicator functions provides a more accurate representation of weekly and hourly seasonality in electricity spot prices. Therefore, the seasonality function Λ has the form

$$\Lambda(t) = A_0 + A_1 t + A_2 \cos\left(\frac{A_3 + 2\pi t}{365 \times 24}\right) + \sum_{i=0}^6 \sum_{h=0}^{23} A_{d,h} \cdot \chi_{d,h}(t), \quad (3)$$

where $A_0, A_1, A_2, A_3, A_{d,h}$ are parameters which need to be estimated.

Stochastic process P

Many stochastic models have been proposed to represent the uncertainty of electricity prices. Among these, factor models stand out as a robust option, offering the advantage of modelling key stylized features like mean reversion, jumps, spikes and negative prices in a flexible and tractable framework [DFG21, MBT08]. Therefore, we follow the approach of [MBT08] and adopt a two-factor model for the deseasonalized spot price. Therefore P has the form

$$P(t) = P_1(t) + P_2(t), \quad (4)$$

The dynamics of the two components are described by the following two Ornstein–Uhlenbeck processes:

$$dP_1(t) = \lambda_1(\mu - P_1(t))dt + \sigma dW(t), \quad (5)$$

$$dP_2(t) = -\lambda_2 P_2(t)dt + dL(t), \quad (6)$$

where λ_1 (respectively λ_2) are positive constants representing the speed of mean reversion of P_1 (respectively P_2), μ is the long-term mean of P_1 , σ is the volatility of P_1 , W is a standard Brownian motion, and L represents a compound Poisson process driving the spikes, which is independent of W .

Data and calibration

The price model described in Equation (1) is calibrated using German and Austrian daily electricity spot price data obtained from the ENTSO-E Transparency Platform (<https://newtransparency.entsoe.eu/market/energyPrices>), covering the period from January 1, 2023, to January 1, 2024. For each of the 365 days in this sample, we observe a 24-dimensional vector of hourly prices, yielding a total of 8,758 data points. The calibration procedure follows four steps: estimation of the seasonality parameters, extraction of spikes and a Brownian-driven base component in the deseasonalized spot price, estimation of the parameters for the base component, and estimation of the parameters for the jump process. For more details on the calibration, see Appendix A.

Remark 1 *In our model, spot electricity prices are treated as instantaneous, i.e., at any time t the consumer can buy electricity for the price $S(t)$. This is a simplification compared to the actual European day-ahead market, where prices for all delivery intervals of the following day are typically announced simultaneously at 12:45 pm CET on the preceding day. We adopt this assumption to maintain the tractability of the control problem and to focus on the interplay between battery dynamics and price fluctuations.*

2.2 Battery models

Modern batteries are available in a wide range of types, each constructed from distinct materials and designed using manufacturer-specific technologies. These technologies prioritize various performance metrics, including lifespan, power density, efficiency, cost, and operational reliability. Despite these differences, the underlying internal dynamics governing battery behaviour tend to follow similar structural patterns, with variations primarily driven by the specific parameters

considered. Our objective is to formulate an optimal control policy that is applicable across a broad class of stationary storage batteries. A general framework that captures the essential dynamics of a battery storage device can be considered as

$$\frac{dY(t)}{dt} = F[t, Y, I, V], \quad t \in [0, T], \quad (7)$$

where Y is a state vector of dimension $d_y \in \mathbb{N}$, representing various battery parameters, including the state of charge, state of health, and other relevant internal state of the battery, t the time, and the function F a characteristic of the battery dynamics that captures the electrochemical reactions, underlying physico-chemical processes, and external impacts on the battery system, an depends on the charge and discharge current $I(t)$, and the cell voltage $V(t)$ [V].

The dynamics of the battery is described by the battery capacity $Q(t)$ [Ah], which reflects the amount of charge a battery can store. This is related to the current $I(t)$ [A] that is flowing into or out of the battery via

$$\frac{dQ(t)}{dt} = I(t), \quad t \in [0, T], \quad (8)$$

which is essentially the conservation of charge. We assume that $Q(t) \in [0, Q_0^{\max}]$, where Q_0^{\max} is the initial maximum capacity, and decompose

$$I(t) = C(t) \cdot I_C^1 \quad \text{where} \quad I_C^1 := \frac{Q_0^{\max}}{1[h]} \quad (9)$$

is the current required to charge the battery in one hour and $C \in [C_{\min}, C_{\max}]$ the C -rate. Note that $C > 0$ correspond to charge, $C < 0$ to discharge and $C = 0$ is the idle state.

We denote by $y^{\text{SOC}}(t) = \frac{Q(t)}{Q_0^{\max}} \in [y_{\min}^{\text{SOC}}, y_{\max}^{\text{SOC}}]$, the status of charge (SOC) of the battery, which is current capacity with respect to its initial maximum capacity Q_0^{\max} , which satisfies

$$\frac{dy^{\text{SOC}}}{dt} = C(t), \quad t \in [0, T]. \quad (10)$$

We will examine in this work two simplistic classes of battery models in our combined optimal control problem but mention here, that general models of the type (7) can in general be applied.

Battery model 0

We denote with *model 0* the most simplistic model for a battery, which assumes a constant battery voltage V_{avg} [V] and the SOC y^{SOC} as control variable.

The SOC of the battery is determined by (10) and the model implies that at each time $t \in [0, T]$ the SOC must satisfy $y^{\text{SOC}}(t) \in [y_{\min}^{\text{SOC}}, y_{\max}^{\text{SOC}}]$, where y_{\min}^{SOC} and y_{\max}^{SOC} are going to be managed by our optimal control solver.

However, this model has certain limitations, most prominently that a direct measurement of the measuring battery capacity is often impractical in real-world scenarios. Instead, real-world batteries are controlled via voltage measurements, which motivates the next class of battery models.

Battery model 1

Instead of using the SOC as state constraint for battery charging and discharging, we consider in *model 1* the battery voltage V control variable.

The cell voltage V of a battery can be considered as

$$V(y^{\text{SOC}}, t) = V^{\text{OCV}}(y^{\text{SOC}}) + R \cdot C(t) =: \widehat{V}(y^{\text{SOC}}, C). \quad (11)$$

where $V^{\text{OCV}}(y^{\text{SOC}})$ is the open circuit voltage (OCV) of the battery and $R = \widetilde{R} \cdot \frac{Q_0^{\max}}{1[h]}$ the internal resistance. The OCV is the voltage the battery cell delivers under infinitesimal small currents, i.e. $C \rightarrow 0$. The OCV is material and cell specific and a function of the OSC, and various methodologies exist to establish their relationship. In [PSK⁺22], multiple modelling

approaches, including linear regression models, non-linear regression models, and hybrid or piecewise linear regression models, are for instance explored.

Based on criteria such as mean error, complexity, Bayes factor, and others, OCV models are ranked, and among them, we choose to work with a polynomial model [WSP14] where parameters are estimated by non-linear regression, but emphasize that this is not a restriction for our general method.

Within our battery dynamics, the control problem requires that at each time t the voltage satisfies $V(t) \in [V_{\min}, V_{\max}]$. The appropriate upper bound V_{\max} and lower bound V_{\min} , are chosen as constants from the battery operator, reflecting conditions to avoid unwanted side reactions (e.g. lithium plating, copper dissolution, electrolyte oxidation).

It is important to note that when considering voltage constraint, charging the battery at its maximum rate will not allow it to reach the maximum SOC. Instead, the battery gradually reduces its charging rate as it approaches full capacity, which is a more realistic behaviour than assuming continuous SOC constraint. Further details on this behaviour will be discussed subsequently.

Remark 2 *The OCV of a battery can be subject to hysteresis between charging and discharging for various materials. This can be incorporated by a hysteresis function $h(\cdot)$ in the voltage dynamics, as developed in [PSK⁺22].*

2.3 Some useful relations

We define the consumer power demand P_{dmd} (in [W]) as the amount of electricity consumed at a given moment in time. Further, we make the following assumptions:

Assumption 1 *The consumer power demand P_{dmd} is constant.*

In our study, the battery is designed to meet the power demand for a duration of \mathcal{T}_{bat} hours (which refers to the amount of time a battery can continuously supply power to meet a specific demand). It is well noticed that the assumption of a constant power demand is simplistic, as in reality, demand is not constant but can be stochastic, following seasonal patterns similar to those observed in electricity prices. To align consumption with our strategy, we aim to establish a relation between P_{dmd} , the rate of discharge of the battery, and the battery's maximum capacity Q_0^{max} .

Firstly, to determine the battery duration, it is crucial to find the maximum discharge rate at which we can discharge the battery to meet the consumer demand. Therefore, from the relation

$$P_{\text{dmd}} \stackrel{!}{=} P_{\text{bat}} =: I \cdot V = I_C^1 \cdot C \cdot \widehat{V} \leq I_C^1 \cdot C \cdot V_{\max}, \quad (12)$$

we can deduce a strong estimation of the maximum discharge rate of the battery with the relation

$$C_{\text{dis}}^{\text{max}} := \frac{P_{\text{dmd}}}{I_C^1 \cdot V_{\max}} \leq C. \quad (13)$$

Secondly, following the main objective of minimizing the cost of electricity consumption, integrating a battery into our consumption strategy can indeed be advantageous. However, optimizing its maximum capacity is crucial since it is closely related to consumer needs. Specifically, we want to avoid purchasing an oversized battery that results in underutilized capacity or a small battery that cannot meet the consumption requirements. Therefore, we aim to establish a connection between P_{dmd} and Q_0^{max} so that the battery can satisfy the demand for \mathcal{T}_{bat} hours. This relationship is derived from the energy consumed during the period $[0, \mathcal{T}_{\text{bat}}]$. From Assumption 1, we have

$$E_{\text{dmd}}^{\mathcal{T}_{\text{bat}}} := \mathcal{T}_{\text{bat}} \cdot P_{\text{dmd}} \stackrel{!}{=} E_{\text{bat}}^{\mathcal{T}_{\text{bat}}} =: \int_0^{\mathcal{T}_{\text{bat}}} I \cdot \widehat{V} dt = Q_0^{\text{max}} \int_0^{\mathcal{T}_{\text{bat}}} \frac{dy^{\text{SOC}}}{dt} \cdot \widehat{V} dt = Q_0^{\text{max}} \cdot \overline{V}(C).$$

with

$$\overline{V}(C) := \int_{y^{\text{SOC}}(0)}^{y^{\text{SOC}}(\mathcal{T}_{\text{bat}})} \widehat{V}(y, C) dy, \quad (14)$$

which yields

$$Q_0^{\text{max}} = \frac{\mathcal{T}_{\text{bat}} \cdot P_{\text{dmd}}}{\overline{V}(C)}. \quad (15)$$

Equation (15) provides a robust formulation representing the initial maximum capacity of the battery and the consumer demand. While this relation incorporates the average voltage of the battery, for simplicity, a rough approximation of (15) can be considered, given that $\bar{V}(C) \leq V_{\max}$. Therefore, we choose Q_0^{\max} such that:

$$Q_0^{\max} \geq \frac{\mathcal{T}_{\text{bat}} \cdot P_{\text{dmd}}}{V_{\max}}. \quad (16)$$

Hence, the current required to charge or discharge the battery can be expressed as

$$I_C^1 = \frac{Q_0^{\max}}{1[h]} = \frac{\mathcal{T}_{\text{bat}} \cdot P_{\text{dmd}}}{\bar{V}(C) \cdot 1[h]}. \quad (17)$$

and the maximum discharge rate, given by equation (13), can be expressed as

$$C_{\text{dis}}^{\max} := \frac{P_{\text{dmd}}}{I_C^1 \cdot V_{\max}} = \frac{1}{\mathcal{T}_{\text{bat}}} \cdot \frac{\bar{V}(C)}{V_{\max}}. \quad (18)$$

3 Stochastic Optimal Control

Our primary objective is to formulate the optimization problem governing the charging and discharging of the battery. We begin by defining the state constraints associated with the battery. Based on this, we introduce the associated control problem and derive the corresponding optimal policy and value function. This comprehensive framework allows us to determine the optimal control strategies that minimize the electricity consumption cost.

3.1 State dynamics.

We denote by $\mathcal{Y} \subset \mathbb{R}^{d_y}$, $d_y \in \mathbb{N}$, the state space for the battery state dynamics. We also denote by $\mathcal{S} \subset \mathbb{R}^{d_s}$, $d_s \in \mathbb{N}$, the state space for the electricity spot price dynamics. In order to emphasize the influence of the control $C \in [-C_{\min}, C_{\max}] =: \mathcal{C}$, we write the battery state process $Y = Y^C$ which satisfies Equation (7). Likewise, the state price process S satisfies Equation 1.

Since the system dynamics are Markovian, the pair of state variables $(Y^C(t), S(t))$ contains all the informations needed to predict the future evolution. Therefore, the control can be expressed as a function of the present state without loss of generality [How60] and we can write $C(t) = \tilde{C}(t, Y^C(t), S(t))$, $t \in [0, T]$, with $\tilde{C} : [0, T] \times \mathcal{Y} \times \mathcal{S} \rightarrow \mathcal{C}$ as a measurable function. That means, the control at any time t depends only on the current time and on the current state variables.

3.2 State constraint

We require that the battery state process satisfies the state constraint $Y(t) \in \mathcal{Y}$ for all $t \in [0, T]$. We therefore define the set of admissible controls by

$$\mathcal{A}_t^{\text{adm}}(y) := \left\{ \tilde{C} : [t, T] \times \mathcal{Y} \times \mathcal{S} \rightarrow \mathcal{C} \mid Y(t) = y, Y \text{ evolves according to (7), and } Y(\tau) \in \mathcal{Y} \forall \tau \in [t, T] \right\}. \quad (19)$$

Depending on the battery model under consideration, the associated state constraints differ. For battery model 0, the state of charge must remain within the admissible interval $[y_{\min}^{\text{SOC}}, y_{\max}^{\text{SOC}}] =: \mathcal{Y}$. The general procedure is to solve the state equation (7) for a given control $C(t)$ and subsequently verify whether the resulting state satisfies this constraint.

For battery model 1, the admissible state set is further restricted by voltage limits; in addition to the state of charge constraint, the battery voltage must remain within the range $[V_{\min}, V_{\max}]$.

By abuse of notation, we write $C \in \mathcal{A}_t^{\text{adm}}(y)$ to indicate that $C(\tau) = \tilde{C}(\tau, Y(\tau), S(\tau))$ and $\tilde{C} \in \mathcal{A}_t^{\text{adm}}(y)$.

3.3 Objective function

Consider the control process $C = (C(t))_{t \in [0, T]}$, $C(t) \in \mathcal{C}$, the state variable $Y^C(t) = y \in \mathcal{Y}$, the electricity state price $S(t) = s \in \mathcal{S}$ at time $t \in [0, T]$. To give the explicit form of the objective function it is essential to first define the running cost, initial and the terminal cost.

3.3.1 Running costs

The running cost includes the cost of buying electricity from the grid and also the operation cost of the battery. Given a specific time t , the running cost is defined by

$$L(t, y, s, C) = L_{\text{buy}}(t, y, s, C) + L_{\text{op}}(t, y, s, C), \quad (20)$$

for all $C(t) \in \mathcal{C}$. In general, we have $P_{\text{buy}} = P_{\text{dmd}} + P_{\text{bat}}$, where P_{buy} is the electrical power we buy from the market. If the electricity spot price at time t is $S(t) = s \left[\frac{\text{€}}{\text{MWh}} \right]$ then, the cost of purchasing electricity is given by

$$\begin{aligned} L_{\text{buy}}(t, y, s, C) &= s \cdot P_{\text{buy}} = s (P_{\text{dmd}} + P_{\text{bat}}) = s (P_{\text{dmd}} + I_C^1 \cdot C(t) \cdot V(y, t)) \\ &= s \left(P_{\text{dmd}} \left(1 + \frac{\mathcal{T}_{\text{bat}}}{1[h]} C(t) \cdot \frac{V(y, t)}{\bar{V}(C)} \right) \right). \end{aligned}$$

The operation of energy storage systems through charging and discharging requires accounting for several cost components associated with their use. These typically include operational, maintenance, and cooling costs [MVB⁺20], which can often be time dependent [Eur24]. In this work, we focus on the operational cost component L_{op} , which is modelled as an additional consumption cost increasing proportionally with the level of the control action, regardless of whether the battery is charging or discharging. L_{op} is defined by the following expression:

$$L_{\text{op}}(t, y, s, C) = s \cdot P_c |P_{\text{bat}}| = s \cdot P_c |I_C^1 \cdot C(t) \cdot V(y, t)| = s \cdot P_c \left| \frac{\mathcal{T}_{\text{bat}} \cdot P_{\text{dmd}}}{1[h]} \cdot C(t) \cdot \frac{V(y, t)}{\bar{V}(C)} \right|.$$

Here, P_c represents the unit operational cost associated with the use of the battery. To ensure the linear dependency of $L_{\text{op}}(\cdot)$ in P_{dmd} . Let us denote by \bar{L} the normalized running cost or unit cost (cost per unit of demand) such that:

$$\bar{L}(\cdot) = \frac{L_{\text{buy}}(\cdot)}{P_{\text{dmd}}} + \frac{L_{\text{op}}(\cdot)}{P_{\text{dmd}}}, \quad (21)$$

3.3.2 Initial and terminal cost

The initial cost Φ^0 corresponds to the cost of purchasing and installing a battery at the unit price of $s_{\text{bat}}^{\text{unit}}(t_0)$ and it is defined by

$$\Phi^0 = s_{\text{bat}}^{\text{unit}}(t_0) \cdot Q_0^{\text{max}} = P_{\text{dmd}} \left(s_{\text{bat}}^{\text{unit}}(t_0) \cdot \frac{\mathcal{T}_{\text{bat}}}{\bar{V}(C)} \right). \quad (22)$$

The terminal cost is a function Φ^T depending on the battery state variable and the electricity price state at the time horizon. The specific form of this function depends on the phenomena that we aim to model at the terminal time. In our setting, we assume that it is a combination of the cost of reselling the battery at the price $s_{\text{bat}}^{\text{unit}}(T)$ and the liquidation cost (cost of selling the power left in the battery at terminal time T). An explicit form of the function is given by:

$$\begin{aligned} \Phi^T(y, s) &= -s_{\text{bat}}^{\text{unit}}(T) \cdot Q_T^{\text{max}} - s \cdot Q_T \\ &= -P_{\text{dmd}} \left(\frac{s_{\text{bat}}^{\text{unit}}(T) \cdot \mathcal{T}_{\text{bat}} + s(T) \cdot y^{\text{SOC}}(T) \cdot \mathcal{T}_{\text{bat}}}{\bar{V}(C)} \right). \end{aligned} \quad (23)$$

We also denote by $\bar{\Phi}^0$ (respectively $\bar{\Phi}^T$) the normalized initial (respectively terminal) cost such that

$$\bar{\Phi}^0 = \frac{\Phi^0}{P_{\text{dmd}}} \quad \text{and} \quad \bar{\Phi}^T(\cdot) = \frac{\Phi^T(\cdot)}{P_{\text{dmd}}}. \quad (24)$$

3.3.3 Cost function

The cost function at time t denoted $J : [0, T] \times \mathcal{Y} \times \mathcal{S} \times \mathcal{C} \rightarrow \mathbb{R}$ is the expected aggregated discounted cost over the time period $[t, T]$ and explicitly defined by

$$J(t, y, s; C) = \mathbb{E} \left[\int_t^T e^{-r(\tau-t)} \bar{L}(\tau, Y^C(\tau), S(\tau), C(\tau)) d\tau + e^{-r(T-t)} \left(\bar{\Phi}^T(Y^C(T), S(T)) + \bar{\Phi}^0 \right) \middle| Y^C(t) = y, S(t) = s \right] \quad (25)$$

Here, $r \geq 0$ denotes the discount rate, $\bar{L}(\cdot)$ is the running cost defined by (21), $\bar{\Phi}^0$ and $\bar{\Phi}^T(\cdot)$ the initial and terminal cost defined by (24). Since battery degradation is not considered in our model, the maximum battery's capacity remains unchanged between the initial time t_0 and the terminal time T . Therefore, we assume that $s_{\text{bat}}^{\text{unit}}(t_0) = s_{\text{bat}}^{\text{unit}}(T)$, so that the total terminal cost $\bar{\Phi}^T(Y^C(T), S(T)) + \bar{\Phi}^0$ reduces to the liquidation cost only.

Our goal is to minimize the performance criterion (25) over the set of all admissible controls $\mathcal{A}_t^{\text{adm}}(y)$. We defined the value function for all $(t, y, s) \in [0, T] \times \mathcal{Y} \times \mathcal{S}$ by

$$U(t, y, s) = \inf_{C \in \mathcal{A}_t^{\text{adm}}(y)} J(t, y, s; C). \quad (26)$$

To solve (26), we first approximate the continuous time problem by a discrete time formulation and then apply Monte Carlo simulation combined with dynamic programming to compute an approximate solution.

4 Numerical approximation

Let T be a finite time horizon, we define the discrete time points $t_k = k \cdot \Delta t$, $k = 0, \dots, N$, where $N \in \mathbb{N}$ is the number of time steps and $\Delta t = \frac{T}{N} = t_{k+1} - t_k$ is the step size.

Short hand notation: We denote by $Y_k = Y(t_k)$ (respectively $S_k = S(t_k)$) the short hand notation for the battery state process (respectively the electricity price process) at time t_k , and $C_k = C(t_k)$ the decision rule at time t_k .

We assume that during the time period $[t_k, t_{k+1})$, the control C_k is given and is constant. Y_k and S_k are given and serve as initial conditions to respectively solve the battery state equation (7) and electricity price equation (1) in $[t_k, t_{k+1}]$. The output of this procedure comprises the updated battery and electricity price state variables at time t_{k+1} for all potential controls $C(t_k)$. Moreover, the class of admissible controls $\mathcal{A}_k^{\text{adm}}$ at time t_k consists of controls C_k such that the state Y_k takes values at any time in \mathcal{Y} . i.e.,

$$\mathcal{A}_k^{\text{adm}}(y) := \left\{ \tilde{C} : [t_k, t_N] \times \mathcal{Y} \times \mathcal{S} \rightarrow \mathcal{C} \mid Y_k = y, Y \text{ evolves according to (7), and } Y_\tau \in \mathcal{Y} \forall \tau = k, \dots, N-1 \right\}. \quad (27)$$

Now, given a control process $C = (C_k)_{k=0, \dots, N-1}$, the cost function $J : \{0, 1, \dots, N\} \times \mathcal{Y} \times \mathcal{S} \times \mathcal{C} \rightarrow \mathbb{R}$ is the expected aggregated cost over the time $k = 0, 1, \dots, N$ defined by

$$J_k(y, s; C) = \mathbb{E} \left[\sum_{l=k}^{N-1} e^{-r(t_l - t_k)} \bar{L}_l(Y_l^C, S_l, C_l) + e^{-r(T - t_k)} \left(\bar{\Phi}^T(Y_N^C, S_N) + \bar{\Phi}^0 \right) \mid Y_k^C = y, S_k = s \right], \quad (28)$$

for all $(y, s) \in \mathcal{Y} \times \mathcal{S}$. The running cost \bar{L} is given by (20), the initial and the terminal cost $\bar{\Phi}^0$, $\bar{\Phi}^T$ by (24). The goal is to minimize the performance criterion (28) over the set of all admissible controls. Therefore, we defined the value function for all $(y, s) \in \mathcal{Y} \times \mathcal{S}$ and $k = 0, 1, \dots, N$ by

$$U_k(y, s) = \inf_{C \in \mathcal{A}_k^{\text{adm}}(y)} J_k(y, s; C). \quad (29)$$

A control $C^* \in \mathcal{A}_k^{\text{adm}}(y)$ is called optimal control if $U_k(y, s) = J_k(y, s; C^*)$.

4.1 Dynamic programming equation

Our control problem has to satisfies the following necessary optimality condition called Bellman equation or Dynamic programming equation, see [BR11],

$$\begin{cases} U_k(y, s) = \inf_{C \in \mathcal{A}_k^{\text{adm}}(y)} \left\{ \bar{L}_k(y, s, C) + e^{-r(t_{k+1} - t_k)} \mathbb{E} \left[U_{k+1}(Y_{k+1}^c, S_{k+1}) \mid Y_k^C = y, S_k = s \right] \right\}, \\ U_N(y, s) = \bar{\Phi}^T(y, s) + \bar{\Phi}^0, \end{cases} \quad (30)$$

for $k = 0, 1, \dots, N-1$ and $(y, s) \in \mathcal{Y} \times \mathcal{S}$. The ideal candidate for the optimal control is $C_k^* = \tilde{C}_k^*(Y_k^C, S_k)$, such that the decision rule satisfies

$$\tilde{C}_k^*(y, s) \in \operatorname{argmin}_{C \in \mathcal{A}_k^{\text{adm}}(y)} \left\{ \bar{L}_k(y, s, C) + \mathbb{E} \left[U_{k+1}(Y_{k+1}^c, S_{k+1}) \mid Y_k^C = y, S_k = s \right] \right\}, \quad (31)$$

for $(y, s) \in \mathcal{Y} \times \mathcal{S}$, $k = 0, 1, \dots, N - 1$.

Next, we introduce the least squares Monte Carlo method, which facilitates efficient numerical solutions for our discrete problem. The core concept involves simulating a series of trajectories and subsequently applying a dynamic programming formulation, specifically the Bellman equation. This enables the recursive computation of value function and optimal decision estimates using least squares regression.

4.2 Least squares Monte Carlo method

The computation of the conditional expectation in the Bellman equation constitutes the main challenge in this case. Before addressing this issue, let us first define the following function.

$$w_k(y, s) := \mathbb{E} \left[U_{k+1}(\varphi_{k+1}(y, C_k), S_{k+1}) \middle| S_k = s \right], \quad (y, s) \in \mathcal{Y} \times \mathcal{S}, \quad \text{for } 0 \leq k \leq N - 1. \quad (32)$$

Here $\varphi_{k+1}(y, C_k) = Y_{k+1}^C$, is the update rule, meaning that given a control C_k and the state $Y_k^C = y$, $\varphi_{k+1}(y, C_k)$ returns the next state at time t_{k+1} . Then, the Bellman equation (30) can be written as

$$\begin{cases} U_k(y, s) = \inf_{C \in \mathcal{A}_k^{\text{adm}}(y)} [\bar{L}_k(y, s, C) + e^{-r(t_{k+1}-t_k)} w_k(y, s)], & 0 \leq k \leq N - 1, \\ U_N(y, s) = \bar{\Phi}^T(y, s) + \bar{\Phi}^0. \end{cases} \quad (33)$$

In the following, we explore the use of least squares regression to approximate the function w_k . Therefore, let $\{\psi_1, \dots, \psi_p\}$ with $\psi_j : \mathcal{S} \rightarrow \mathbb{R}$, $j = 1, \dots, p$, be a set of basis functions, then we write $\psi(s) = (\psi_1(s), \dots, \psi_p(s))$. Let $(\hat{U}_k)_{k=0}^N$ denotes the sequence of approximated value functions and set $\hat{U}_N = \bar{\Phi}^T(y, s) + \bar{\Phi}^0$. Then, we estimate \hat{U}_k recursively as follows. For a fixed $y \in \mathcal{Y}$ and given the approximated value function \hat{U}_{k+1} , we approximate the function w_k by

$$\hat{w}_k(y, s) := \sum_{j=1}^p \beta_{k,j}^{(y)} \psi_j(s), \quad (34)$$

where the regression coefficients $\beta_k^{(y)} = (\beta_{k,1}^{(y)}, \dots, \beta_{k,p}^{(y)})^T$ are solutions of the least squares problem

$$\beta_{k,1}^{(y)}, \dots, \beta_{k,p}^{(y)} := \arg \min_{\beta_1, \dots, \beta_p} \frac{1}{N_{\text{train}}} \sum_{m=1}^{N_{\text{train}}} \left| \hat{U}_{k+1}(\varphi_{k+1}(y, C_k), S_{k+1}^{(m)}) - \sum_{j=1}^p \beta_{k,j}^{(y)} \psi_j(S_k^{(m)}) \right|^2. \quad (35)$$

Here, $(S_k^{(m)})_{k=0}^N$, $m = 1, \dots, N_{\text{train}}$, are $N_{\text{train}} \in \mathbb{N}$ independent trajectories sampled from the underlying state process $(S_k)_{k=0}^N$. Afterwards, the corresponding (approximated) value function is then given by

$$\hat{U}_k(y, s) = \min_{C \in \mathcal{A}_k^{\text{adm}}(y)} [\bar{L}_k(y, s, C) + e^{-r(t_{k+1}-t_k)} \hat{w}_k(y, s)], \quad 0 \leq k \leq N - 1, \quad (36)$$

for $(y, s) \in \mathcal{Y} \times \mathcal{S}$. It is important to note that the choice of basis functions ψ for the regression technique significantly affects its performance, and the class of polynomials is a common option.

To compute the optimal policy C^* , we use the least squares Monte Carlo approach described previously and the procedure is summarized in Algorithm 1. After computing the optimal policy C^* as described in Algorithm 1, we estimate the value $J_0(y_0, S_0; C^*)$ using Monte Carlo method. This estimated value is denoted by $\tilde{J}_0^{C^*}(y_0, S_0)$, and it is obtained by averaging the expected values over N_{test} independent sample paths. The overall procedure is summarized in Algorithm 2. The estimated consumption cost $\tilde{J}_0^{C^*}(y_0, S_0)$ satisfies

$$\mathbb{E} [\tilde{J}_0^{C^*}(y_0, S_0)] \leq \mathbb{E} [U_0(y_0, S_0)]. \quad (37)$$

In other words, $\tilde{J}_0^{C^*}(y_0, S_0)$ provides a *lower bound* for the value function. In the numerical results, we use these estimates to compare the performance for different battery model configurations.

Remark 3 During the numerical simulation, instead of computing the regression for $\widehat{U}_{k+1}(\varphi_{k+1}(y, C_k), S_{k+1}^{(m)})$ in Algorithm 1, we employ $\widehat{U}_{k+1}(y, S_{k+1}^{(m)})$ and obtain an approximation from which $\widehat{w}_k(y, s)$ is computed via linear interpolation. This approach for approximating the conditional expectation is computationally less expensive than direct estimation as presented in Algorithm 1 while yielding nearly identical results, which motivated our choice.

Algorithm 1 Optimal Policy C^*

Simulate M independent sample price trajectories $(S_0^{(m)}, S_1^{(m)}, \dots, S_N^{(m)})_{m=1}^{N_{\text{train}}}$ and **set the terminal solution**

$$\widehat{U}_N(y, S_N^{(m)}) = \overline{\Phi}^T(y, S_N^{(m)}) + \overline{\Phi}^0, \quad y \in \widetilde{\mathcal{Y}} \subset \mathcal{Y}$$

for $k = N - 1$ to 0 (backward in time) **do**

for $y \in \widetilde{\mathcal{Y}}$ **do:**

$$\beta_{k,1}^{(y)}, \dots, \beta_{k,p}^{(y)} = \arg \min_{\beta_1, \dots, \beta_p} \frac{1}{N_{\text{train}}} \sum_{m=1}^{N_{\text{train}}} \left| \widehat{U}_{k+1}(\varphi_{k+1}(y, C_k), S_{k+1}^{(m)}) - \sum_{j=1}^p \beta_{k,j}^{(y)} \psi_j(S_k^{(m)}) \right|^2.$$

$$\widehat{w}_k(y, s) = \sum_{j=1}^p \beta_{k,j}^{(y)} \psi_j(s).$$

end for

 Compute the optimal policy for all $m = 1$ to N_{train} and $y \in \widetilde{\mathcal{Y}}$:

$$C_k^*(y, S_k^{(m)}) = \arg \min_{C_k \in \mathcal{A}_k^{\text{adm}}(y)} \left[\overline{L}_k(y, S_k^{(m)}, C_k) + \widehat{w}_k(y, S_k^{(m)}) \right].$$

 Compute the value function $m = 1$ to N_{train} and $y \in \widetilde{\mathcal{Y}}$:

$$\widehat{U}_k(y, S_k^{(m)}) = \overline{L}_k(y, S_k^{(m)}, C_k^*) + \widehat{w}_k(y, S_k^{(m)})$$

end for

Construct an extension \widehat{C}^* of C^* , $\widehat{C}^* : \widetilde{\mathcal{Y}} \times \mathcal{S} \rightarrow \mathcal{C}$, **such that**

$$\widehat{C}^*(\tilde{y}, s) = f_{\text{interpolate}}(\tilde{y}, s; C_k^*(y, S_k^{(m)}) : y \in \widetilde{\mathcal{Y}}); \quad (\tilde{y}, s) \in \widetilde{\mathcal{Y}} \times \mathcal{S}$$

Algorithm 2 Lower Bound Estimate of $J^{C^*}(t = 0, y_0, S_0)$

Simulate N_{test} independent sample price trajectories: $(S_k'^{(m)})_{k=0}^N$, $m = 1, \dots, N_{\text{test}}$ where S_0' is different from S_0 used in the training samples.

Initialize the state: $y_0 \in \mathcal{Y}$.

for $m = 1, \dots, M_{\text{test}}$ **do**

 Compute the process $(Y_k^{C^*,(m)})_{k=0}^N$, with initial control $y_0 \in \mathcal{Y}$ using:

$$Y_0^{C^*,(m)} = y_0 \quad \text{and} \quad Y_{k+1}^{C^*,(m)} = \varphi_{k+1}(Y_k^{C^*,(m)}, \widehat{C}_k^*(Y_k^{C^*,(m)}, S_k'^{(m)})),$$

end for

Estimate $J^{C^*}(t = 0, y_0, S_0)$ **using the Monte Carlo formulation:**

$$\begin{aligned} \widetilde{J}^{C^*}(t = 0, y_0, S_0) := & \frac{1}{N_{\text{test}}} \sum_{m=1}^{N_{\text{test}}} \left(\sum_{k=0}^{N-1} \overline{L}_k(Y_k^{C^*,(m)}, S_k'^{(m)}, \widehat{C}_k^*(Y_k^{C^*,(m)}, S_k'^{(m)})) \right. \\ & \left. + \Phi^T(Y_N^{C^*,(m)}, S_N'^{(m)}) + \overline{\Phi}^0 \right). \end{aligned}$$

5 Numerical Results

This section is dedicated to exploring numerical results related to the optimal control problem presented previously. Specifically, we will investigate the two models described earlier. We aim to analyse the cost effectiveness of a battery system over a period of up to 10 years, as well as to determine its amortization time. Before proceeding with the full computations, it is essential to select reliable parameters, in particular the state of charge discretization number N_y , the time step Δt (in hour), and the number of Monte Carlo samples. This motivates the Section 5.1, which will be dedicated to identifying suitable choices of these parameters by evaluating the relative error associated with them. To reduce computational effort

in this preliminary study, we restrict ourselves to a time horizon of one year, assuming a battery with a battery duration of 24 hours.

Firstly, we assume that the electricity spot price state variable is a one dimensional process, meaning we only take into account the electricity price $S(t)$ satisfying (1), with seasonality $\Lambda(t)$ following Equation (3) and the stochastic process $P(t)$ following (4). The calibration is well detailed in Appendix A.1.

Secondly, for both battery models 0 and 1, the only state considered is the state of charge. The C-rate is assumed to be between $[-1, 1]$, meaning that we can fully charge or discharge the battery in 1 hour at the maximum speed rate. The state of charge by definition is within the bound $[y_{\min}^{\text{SOC}}, y_{\max}^{\text{SOC}}] = [0, 1]$. For the Battery model 0, the constant voltage is assumed to be the mean value of the voltage. To model the voltage as a function of the SOC, we use the OCV parameters from the polynomial model estimated in [BJM⁺17]. The coefficients of the model are given by: $k_0 = 3.426$, $k_1 = 0.0284$, $k_2 = -0.00128$, $k_3 = 3.14 \cdot 10^{-5}$, $k_4 = -4.1 \cdot 10^{-7}$, $k_5 = 2.83 \cdot 10^{-9}$, $k_6 = -8.1 \cdot 10^{-12}$. Those parameters are obtained after several experiments on a battery cell with a nominal capacity of $Q_0^{\text{max}} = 20$ [Ah] and internal resistance of $\tilde{R} = 0.07$ [Ω] which implies $R = 0.14$ [V]. We also assume that the SBSB satisfies the demand within a range of megawatt-hours (MWh).

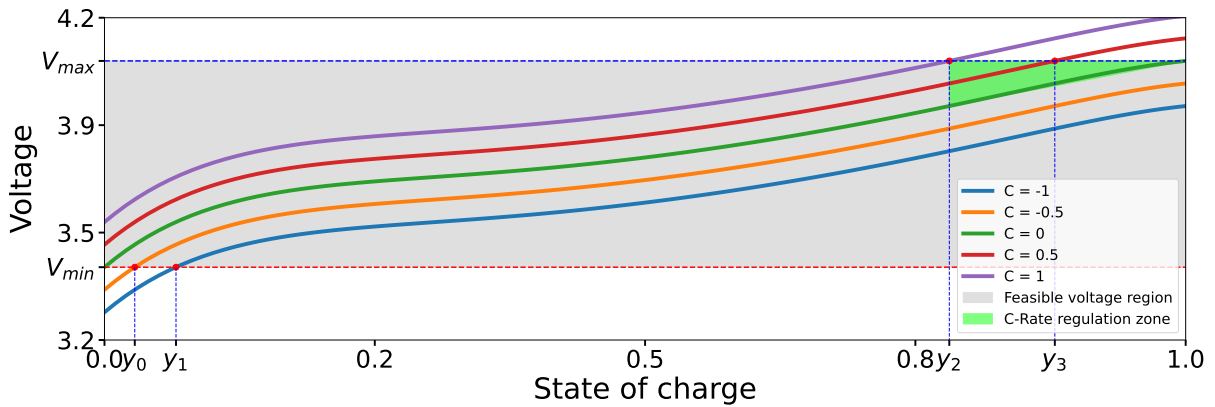


Figure 1: Cell's Voltage vs State of charge for different C-rate and internal resistance of $R = 0.14$.

Figure 1 illustrates the voltage of a cell as a function of SOC and the control C . The shaded region represents the zone where $\hat{V}(y^{\text{SOC}}, C) \in [V_{\min}, V_{\max}]$; every C-rate in that zone is called admissible control. Further, the maximum voltage is achieved at $y^{\text{SOC}} = 1$ and $C = 0$, and the minimum voltage occurs at $y^{\text{SOC}} = 0$ and $C = 0$. The C-rate regulation zone illustrates the contrast between the two battery representations, namely model 0, constrained by the state of charge, and model 1, constrained by the terminal voltage. Under state of charge constraint, the battery can be charged to its full capacity even at a relatively high C-rate. In contrast, in the voltage constrained case, as shown in Figure 1, the terminal voltage reaches its upper limit before the battery attains full charge. This behaviour implies that, as will be discussed in the following sections, the optimal control strategy must gradually decrease the C-rate as the battery approaches its maximum SOC, thereby achieving full charge without exceeding the voltage constraint.

5.1 Preliminary error analysis and parameter selection

For the error analysis, since battery model 0 is obtained under the assumption of constant voltage, we emphasize that only battery model 1 will be used, since it is more general than model 0. Firstly, we establish a reference value for the lower bound $\tilde{J}_0^{C^*}(y_0, S_0)$, since the exact solution is not available. The reference is determined by refining the computation of $\tilde{J}_0^{C^*}(y_0, S_0)$ until further refinement produces only negligible changes in the result. For this purpose, we compute the reference value $\tilde{J}_{0,\text{ref}}^{C^*}(y_0, S_0)$ using the following parameters: time step $\Delta t = 0.1$ hour, state of charge discretization $N_y = 128$, number of training samples $N_{\text{train}} = 10^3$, and number of testing samples $N_{\text{test}} = 2 \cdot 10^4$. The battery duration is set to $\mathcal{T}_{\text{bat}} = 24$ hours with a penalization constant $P_c = 0.001$. The time horizon is $T = 24 \cdot 365$ hours, starting with an empty battery (state of charge $y_0^{\text{SOC}} = 0$) and an initial electricity price of $S_0 = 30$. The corresponding reference values is given by.

$$\tilde{J}_{0,\text{ref}}^{C^*}(y_0, S_0) = 639734.4 \pm 589.049. \quad (38)$$

Here, 589.049 represents the half-length of the estimated 99% confidence interval (40). Afterward, we analyse the behaviour of the relative error ε_r , defined as

$$\varepsilon_r := \frac{\left| \tilde{J}_0^{C^*}(y_0, S_0) - \tilde{J}_{0,\text{ref}}^{C^*}(y_0, S_0) \right|}{\left| \tilde{J}_{0,\text{ref}}^{C^*}(y_0, S_0) \right|}. \quad (39)$$

For each parameter N_y , Δt , N_{train} , and N_{test} , we compute $\tilde{J}_0^{C^*}(y_0, S_0)$ and evaluate the associated sampling uncertainty. Denoting by Std the empirical standard deviation of the estimator based on N_{test} samples, the 99% confidence interval (CI) for the relative error is defined as

$$\left[\varepsilon_r - z \cdot \frac{Std}{\sqrt{N_{\text{test}} \left| \tilde{J}_{0,\text{ref}}^{C^*} \right|}}, \varepsilon_r + z \cdot \frac{Std}{\sqrt{N_{\text{test}} \left| \tilde{J}_{0,\text{ref}}^{C^*} \right|}} \right], \quad (40)$$

where $z \approx 2.576$ for 99% CI is the critical value. Setting an error tolerance of ε_{tol} , the upper bound of the CI should satisfy the relation

$$\varepsilon_r + z \cdot \frac{Std}{\sqrt{N_{\text{test}} \left| \tilde{J}_{0,\text{ref}}^{C^*} \right|}} \leq \varepsilon_{\text{tol}}. \quad (41)$$

To select the parameters that meet this relative error criterion, for each candidate value of a parameter, we retain the largest (or most computationally efficient) choice that still satisfies condition (41).

Now, we start the analysis with the SOC discretization N_y .

N_y	2	4	8	16	32	64
$\tilde{J}_0^{C^*}$	754400.40	664679.75	648368.00	642280.90	640328.10	639828.75
Std	24448.309	31163.576	32005.275	32248.213	32349.059	32388.785
MC error	444.290	566.324	581.620	586.035	587.867	588.589
ε_r	$1.792 \cdot 10^{-01}$	$3.900 \cdot 10^{-02}$	$1.350 \cdot 10^{-02}$	$4.000 \cdot 10^{-03}$	$9.0 \cdot 10^{-04}$	$1.000 \cdot 10^{-04}$

Table 1: Lower bound $\tilde{J}_0^{C^*}(y_0, S_0)$ for different SOC discretization N_y , given that $\Delta t = 0.1$, $N_{\text{train}} = 10^3$, $N_{\text{test}} = 2 \cdot 10^4$, $R = 0.14$, $P_c = 0.001$, $\mathcal{T}_{\text{bat}} = 24$ hours, $T = 24 \cdot 365$ hours. The Monte Carlo error (MC error) is defined as the half-length of the estimated 99% confidence interval around $\tilde{J}_0^{C^*}(y_0, S_0)$.

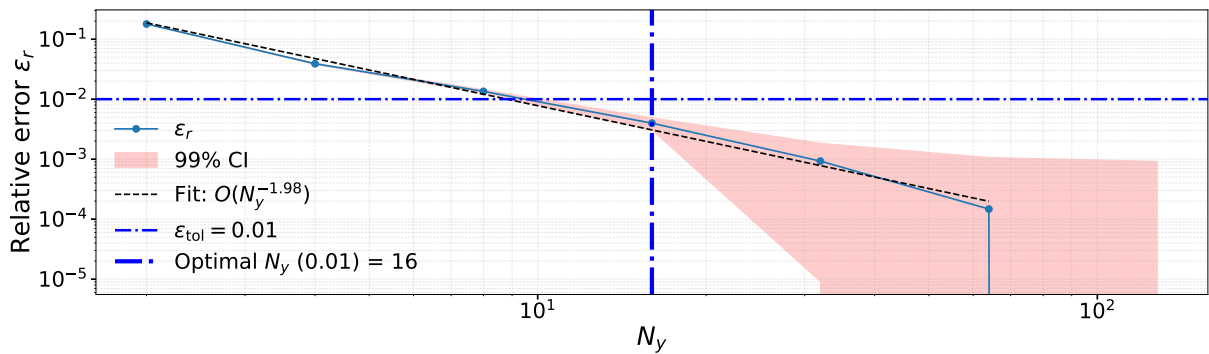


Figure 2: Relative error as function of state of charge discretization N_y .

Table 1 summarizes the numerical results of the consumption cost for various discretization levels N_y . The corresponding standard deviation is approximately 5% of $\tilde{J}_0^{C^*}(y_0, S_0)$. This variability is realistic and consistent with the fluctuations typically observed in electricity market prices. In view of these results, we select a reasonable tolerance threshold of $\varepsilon_{\text{tol}} = 1\%$, corresponding to $N_y = 16$, as shown in Figure 2. This choice provides a reasonable trade-off between numerical accuracy and computational efficiency. However, if the goal is to evaluate the performance limits of the proposed algorithm, a stricter tolerance $\varepsilon_{\text{tol}} = 0.2\%$ would require $N_y = 32$, which is significantly more demanding computationally.

Secondly, we study how the time discretization Δt influences $\tilde{J}_0^{C^*}(y_0, S_0)$.

Δt	1	0.5	0.25	0.125	0.0625	0.01
\tilde{J}_0^{C*}	569711.94	602748.56	626930.06	640778.7	641595.11	642280.9
Std	31317.125	32089.898	32366.926	32278.402	32259.27	32248.213
MC error	560.25	574.08	579.04	577.45	577.15	576.91
ε_r	0.1129	0.0615	0.0239	0.0023	0.0010	-

Table 2: Comparison of the lower bound $\tilde{J}_0^{C*}(y_0, S_0)$ for different time discretization Δt given that $N_y = 16$, $N_{\text{train}} = 10^3$, $N_{\text{test}} = 2 \cdot 10^4$, $R = 0.14$, $P_c = 0.001$, $\mathcal{T}_{\text{bat}} = 24$ hours, $T = 24 \cdot 365$ hours.

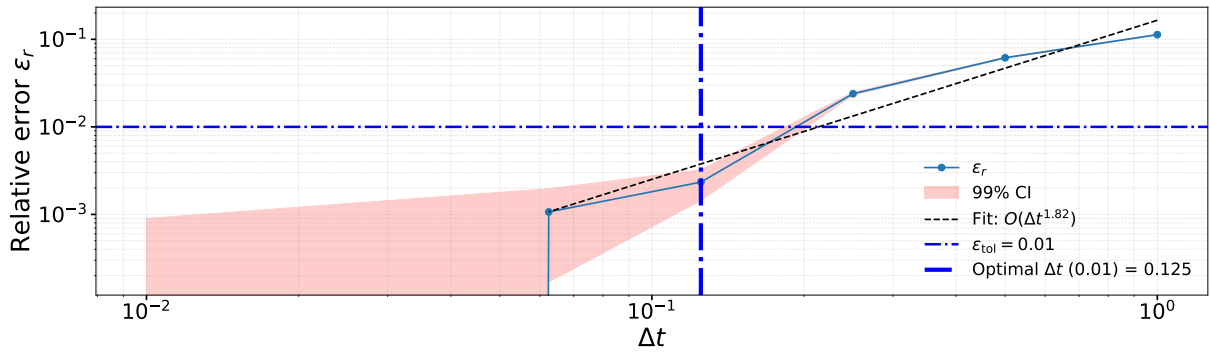


Figure 3: Relative error as function of time step Δt .

In analogy with the previous case, Table 2 summarizes the variations in the computed consumption cost. Under identical tolerance criteria, the discretization step $\Delta t = 0.125$ appears to offer an effective trade-off between numerical accuracy and computational efficiency as illustrate in Figure 3. Finally, we study how the number of testing samples N_{test} for Monte Carlo for the battery state influences $\tilde{J}_0^{C*}(y_0, S_0)$.

N_{test}	1000	2000	4000	8000	16000	32000	64000
\tilde{J}_0^{C*}	640866.420	640813.527	640759.39	640747.73	640457.43	640722.10	640503.50
Std	31760.94	32274.02	32081.90	32151.06	32176.46	32343.74	32407.27
MC error	2541.05	1825.82	1283.36	909.43	643.57	457.44	324.09

Table 3: Comparison of the lower bound $\tilde{J}_0^{C*}(y_0, S_0)$ for different number of sample N_{test} with the following parameters: $\Delta t = 0.1$, $N_y = 128$, $R = 0.14$, $P_c = 0.001$, $\mathcal{T}_{\text{bat}} = 24$ hours, $T = 24 \cdot 365$ hours.

According to Table 3, the Monte Carlo error exhibits the expected behaviour (decreasing as N_{test} increases). The analysis shows that the Monte Carlo method converges at a rate of 0.5. However, our initial choice of $N_{\text{test}} = 2 \cdot 10^4$ samples is a reasonable trade-off between precision and computational cost where the error becomes acceptably low without incurring excessive computational cost.

5.2 Value function and Optimal policy

In this section, we examine how the value function and the optimal policy differ under the two battery models. Our analysis focuses specifically on periods in which the electricity price are high, low prices and in-between. These periods are identified based on the seasonal structure of the price process. For illustration purposes, we restrict the study to a time horizon of three months, which is sufficient to highlight and discuss the qualitative effects of the model differences. From Section 5.1, we will use the following parameters for the upcoming computation, based on the 1% tolerance error; namely: time step $\Delta t = 0.125$ hour, SOC discretisation $N_y = 16$, time horizon $T = 24 \cdot 90$ hours). We $R = 0.14$ and $P_c = 0.01$. Due to seasonality on electricity spot price, we select a representative price interval using quantiles to have a robust result. indeed, this approach removes outliers that could distort the interpretation of the value function, then focus on the central 90% of the distribution and most meaningful part of the price distribution.

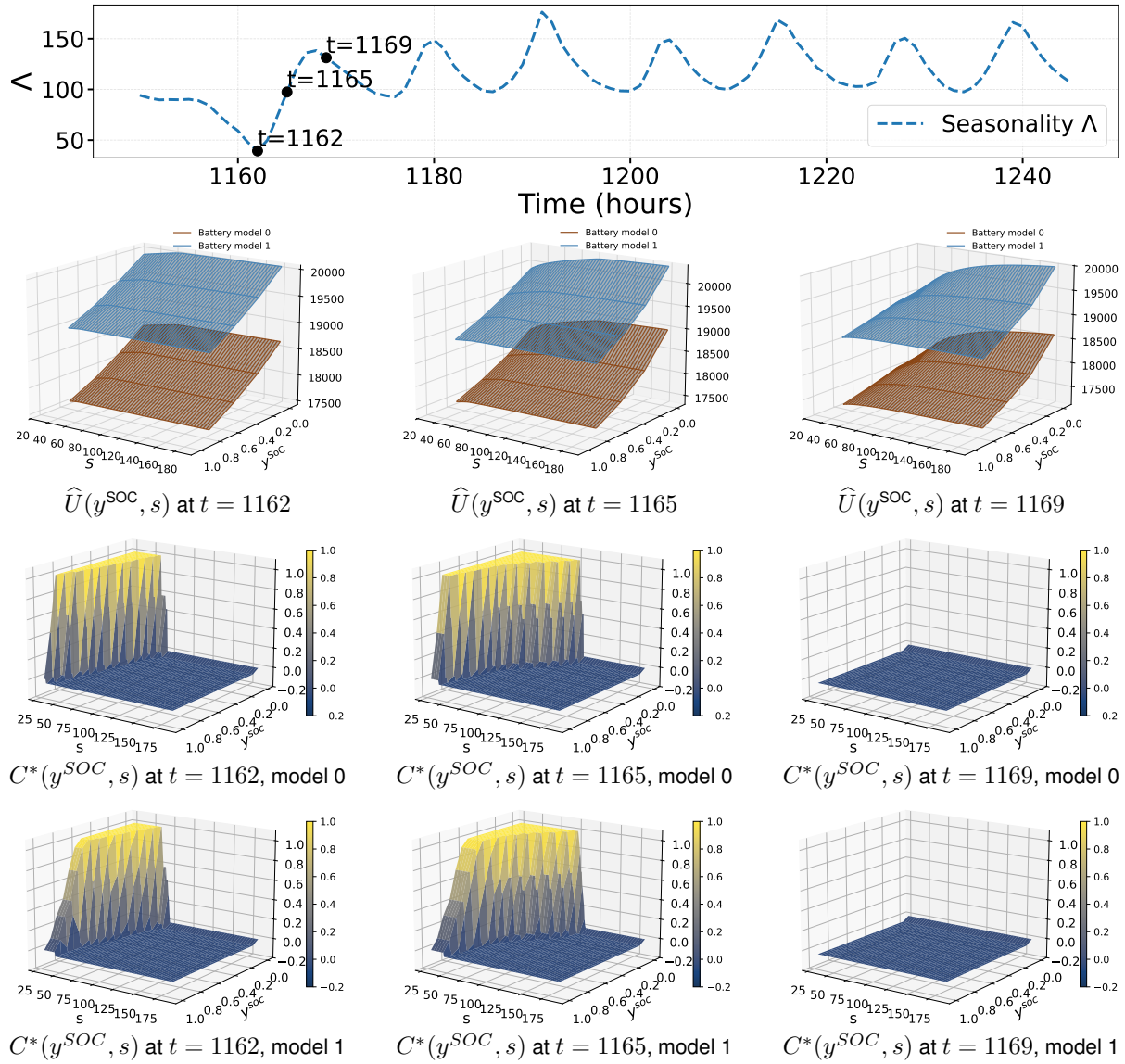


Figure 4: Value functions $\hat{U}(y^{SOC}, s)$ and optimal policy $C^*(y^{SOC}, s)$ under battery model 0 and 1, at different time t (hours)

In Figure 4, we visualize the approximated value function $\hat{U}(y^{SOC}, s)$ and the corresponding optimal policy $C^*(y^{SOC}, s)$ under the two battery models. Here, $\hat{U}(y^{SOC}, s)$ at time t represents the expected consumption cost from time t until the terminal time. We observe that battery model 0 yields a lower expected cost than battery model 1 for all states. This is expected, as model 1 imposes a more conservative behaviour due to voltage constraints, which restrict feasible control actions and consequently increases the expected operational cost. Nonetheless, there may exist specific cases where model 1 leads to a lower cost at a particular time, depending on the sign of $V(y, t) - V_{\text{avg}}$. For both battery models, the optimal policy follows the standard economic principle: charge the battery when the electricity price is low, and discharge when the price is high. For example, at the selected time $t = 1162$, corresponding to a period of very low prices, the optimal strategy is to charge the battery, anticipating a subsequent price increase. As the price begins to increase ($t = 1165$), the optimal control allows the battery to charge at some higher prices, but only if the battery is nearly empty. Conversely, at times of high prices ($t = 1165$), the battery is discharged as much as possible before the price drops again. This pattern repeats over the entire time horizon. Under battery model 1, however, the optimal behaviour is further influenced by the voltage constraint: the C-rate gradually decreases as the battery approaches full charge. This illustrates that model 1 is more restrictive than model 0, and highlights the impact of voltage limitations on operational strategies.

From now on, unless we explicitly study the effect of a specific parameter, all computations will be performed using the following baseline configuration: time step $\Delta t = 0.125$ hours, state of charge discretization $N_y = 16$, time horizon $T = 24 \cdot 365$ hours, internal resistance $R = 0.14$, training sample size $N_{\text{train}} = 10^3$, test sample size $N_{\text{test}} = 2 \cdot 10^4$,

operational constant $P_c = 0.001$, and battery duration $\mathcal{T}_{\text{bat}} = 24$ hours.

5.3 Impact of battery parameters on the consumption cost

In this section, we examine the impact of several key parameters on the consumption cost $\tilde{J}_0^{C^*}(y_0, S_0)$. The parameters under consideration are the battery duration \mathcal{T}_{bat} , the operational constant P_c , and the internal resistance of the battery R . The analysis is carried out under battery model 1. Prior to the analysis, we introduce the quantity η^{save} , which represents the cost savings resulting from the use of the battery and computed using the relation:

$$\eta^{\text{save}} := \frac{J_{0,wb}(S_0) - \tilde{J}_0^{C^*}(y_0, S_0)}{J_{0,wb}(S_0)}. \quad (42)$$

In 42 $J_{wb,0}(S_0)$ denotes the electricity consumption cost when no battery is used. After one year, its estimated value computed via a Monte Carlo simulation using $N_{\text{test}} = 2 \cdot 10^4$ sampled electricity price trajectories is

$$J_{0,wb}(S_0) = 759993.0945 \pm 439.350. \quad (43)$$

We begin with the impact of battery duration on the consumption cost $\tilde{J}_0^{C^*}(y_0, S_0)$. Specifically, we analyse for four different battery duration values i.e. $\mathcal{T}_{\text{bat}} = 1, 6, 12, 24$ and present the result in Table 4, and a visualization of the strategy on a sample price trajectory in Figure 5.

\mathcal{T}_{bat}	1	6	12	24
$\tilde{J}_0^{C^*}$	743169.1	680647.9	663037.5	640778.7
MC error	444.02	496.36	534.59	577.45
η^{save}	0.022	0.104	0.127	0.156

Table 4: Consumption cost $\tilde{J}_0^{C^*}(y_0, S_0)$ and cost savings η^{save} for different battery duration \mathcal{T}_{bat} .

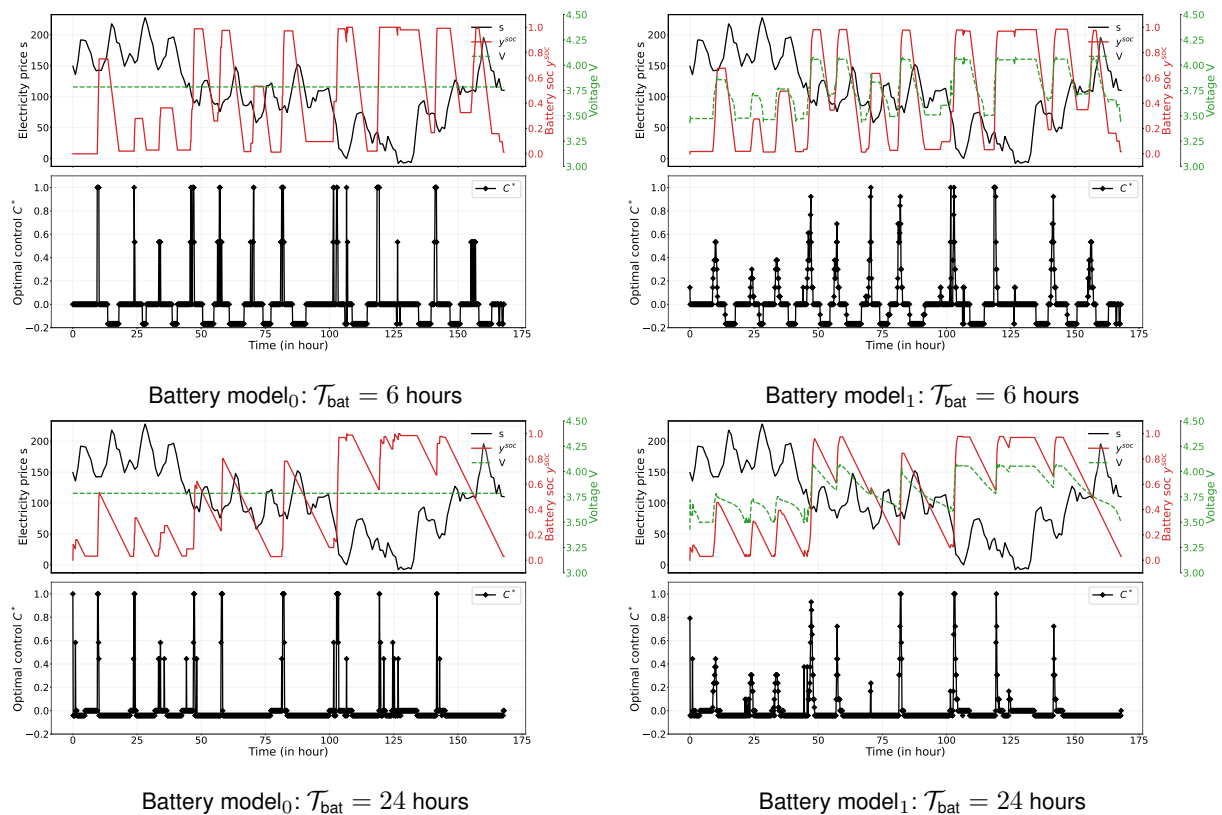


Figure 5: Optimal strategy during a period of one week, for one sample price trajectory given different \mathcal{T}_{bat} , under the battery model 0 (left) and model 1 (right).

We observe that the estimated consumption costs commuted in Table 4 behave as expected. Indeed, the consumption cost decreases when we use larger battery and this leads to greater savings. For instance, after one year, with a battery duration of $\mathcal{T}_{\text{bat}} = 24$ hours, we save up to 15.6% of the consumption cost comparing to the scenario where we don't have a battery. This significant saving is largely due to price fluctuations, as highlighted by Stephan Schlüter et al. in [SDD24]. In Figure 5, we wanted once more to show on trajectory level how the two battery models behave and we observe that under model 0, the battery tends to charge aggressively (with higher C-rate) until it reaches full capacity, showing a "bang-bang" behaviour. In contrast, model 1 regulates the charging process more smoothly, preventing extreme charging rates. This more balanced approach not only optimizes energy use but also helps mitigate battery degradation by avoiding continuous maximum speed charging and it is important to mention that this happens even without considering degradation in the model.

Next, we study the impact of the operational constant P_c on $\tilde{J}_0^{C^*}(y_0, S_0)$. The estimated consumption costs are given in Table 5 for 4 different values ($P_c = 0, 0.1, 0.2, 0.5$) and a visualization of the strategy on a sample price trajectory in Figure 6

P_c	0	0.1	0.2	0.5
$\tilde{J}_0^{C^*}$	640457.3	666059.56	683492.1	712321.6
MC error	586.813	567.7501	551.72	522.140

Table 5: Consumption cost $\tilde{J}_0^{C^*}(y_0, S_0)$ for different operational constant P_c .

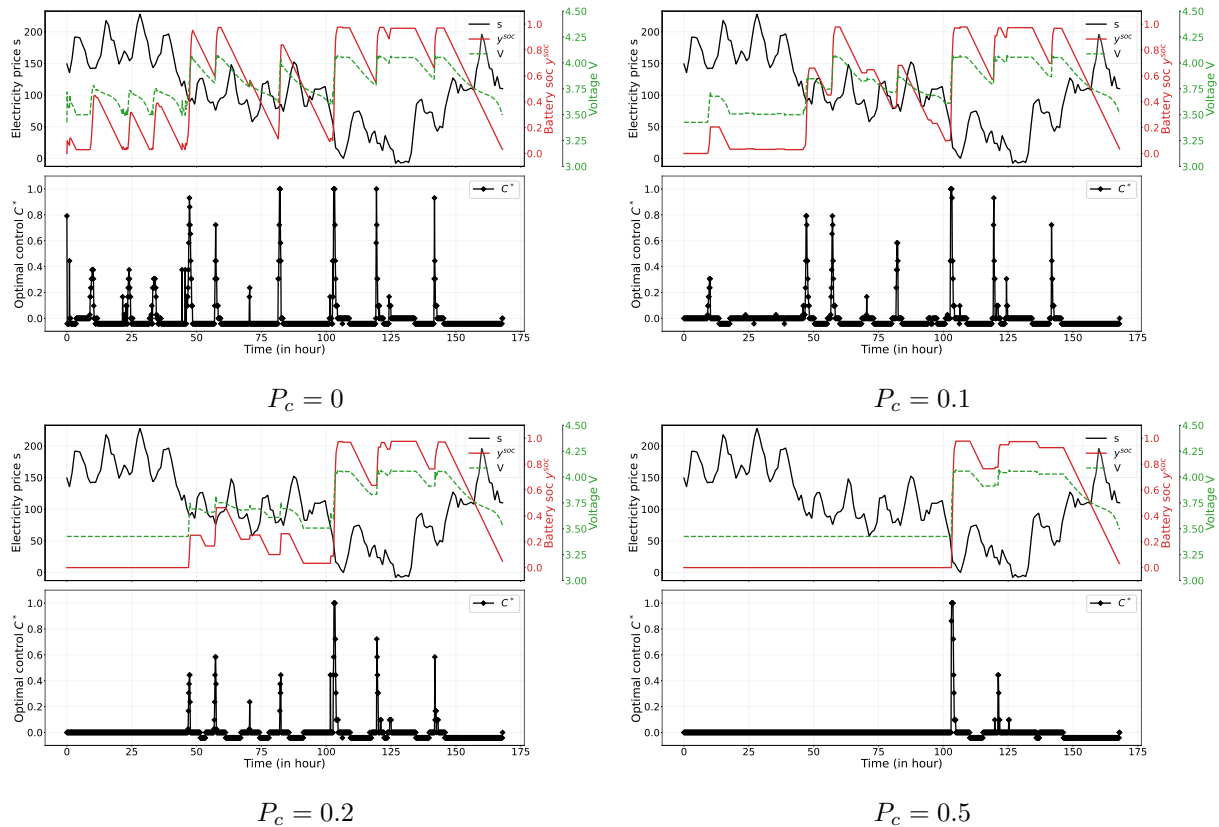


Figure 6: Optimal strategy during a period of one week, for one sample price trajectory given different operational constant P_c .

Table 5 clearly shows that higher values of P_c lead to an increase in the consumption cost. This behaviour is expected, as a larger value of P_c implies a higher operational cost associated with using the battery. Focusing on a sample price trajectory, Figure 6 illustrates how the optimizer reacts to different values of P_c . We observe that, as the operational constant increases, the optimizer becomes less likely to use the battery for every price fluctuation. Instead, the battery is used only when necessary, and for certain electricity spot price trajectories it may even be optimal not to use the battery

at all.

Lastly, we study the impact of the internal resistance R on $\tilde{J}_0^{C^*}(y_0, S_0)$. Particularly, we analyse four different values ($R = 0, 1, 2, 3$). The result are presented in Table 6 and a visualization of the strategy on a sample price trajectory in Figure 7.

R	0	1	2	3
$\tilde{J}_0^{C^*}$	631092.25	639846.0	642214.1	660473.5
MC error	588.88	564.58	526.46	498.75

Table 6: Consumption cost $\tilde{J}_0^{C^*}(y_0, S_0)$ for different internal resistance value R .

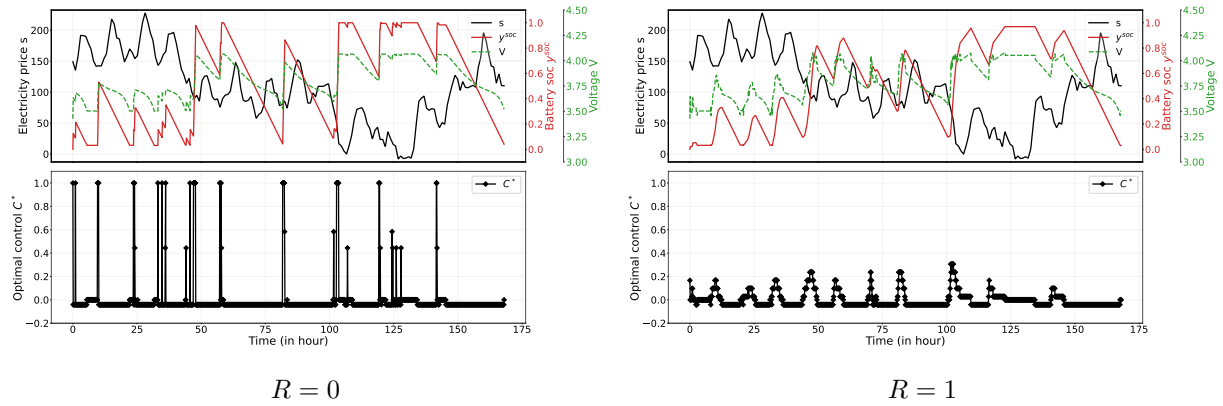


Figure 7: Optimal strategy during a period of one week, for one sample price trajectory given different internal resistance values R .

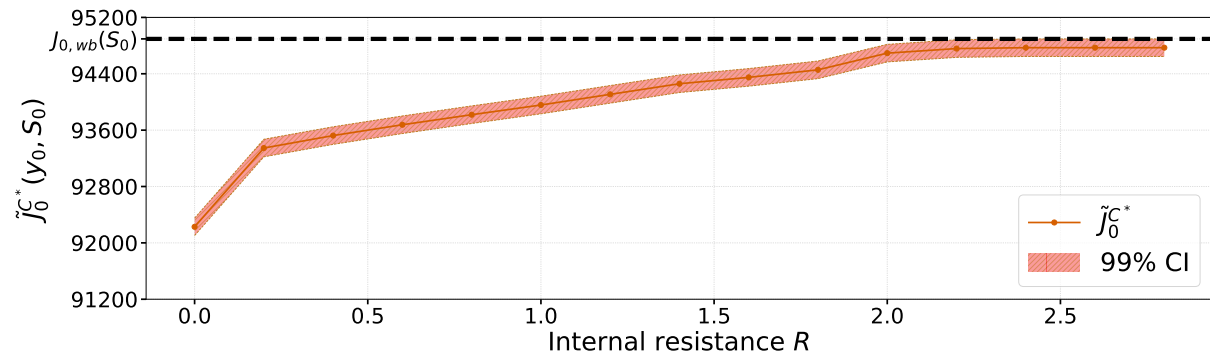


Figure 8: Consumption cost $\tilde{J}_0^{C^*}(y_0, S_0)$ for different internal resistance value R presented in Table 13, for a time horizon of $T = 24 \cdot 30$ hours.

Increasing the internal resistance of the battery reduces the set of admissible actions $\mathcal{A}_t^{adm}(Y^C, S)$ for battery model 1. A higher internal resistance allow the voltage limit to be reached more quickly and certain C-rate values may no longer be admissible. As a result, the battery requires more time to reach full charge, which in turn increases the overall consumption cost, as shown in Table 6 and more deeply in Table 13 for shorter time. In Figure 7, we observe that for smaller values of R , the optimal strategies permit higher C-rates. However, as R increases, the admissible C-rate values progressively diminish. Consequently, when the internal resistance becomes sufficiently large, the optimal strategy converges toward the scenario in which the battery is not utilized at all. This trend is reflected in the consumption cost, which exhibits the same behaviour, as illustrated in Figure 8.

This behaviour is consistent with what is typically observed when degradation effects are incorporated into the battery model through the internal resistance. Indeed, when degradation is modelled, frequent use of the battery leads to an increase in R , and consequently the control must adapt to limit the battery usage in order to mitigate further degradation.

6 Amortization time

The objective of this section is to estimate the amortization time T_a , taking in account the savings percentage η^{save} and the battery duration \mathcal{T}_{bat} . Indeed the amortization time is formally defined as the time when the cumulative savings exceed the initial investment in the battery S_{bat} [€] (the time when using the battery becomes beneficial). i.e.

$$T_a := \inf \left\{ T \mid J_{0,wb}^T(S_0) - \tilde{J}_0^{C^*,T}(y_0, S_0) > S_{\text{bat}} \right\}, \quad (44)$$

Due to the investment cost associated with purchasing and installing the battery, the amortisation time T_a is expected to be reached only after several years. To estimate this time, we run our algorithm over a period of $T = 8$ years, focusing on several values of the battery duration, namely $\mathcal{T}_{\text{bat}} = 6, 12, 24$. Because of computational constraints, we assume that the battery is controlled every $\Delta t = 1$ hour. We also assume according to <https://www.lifepo4prices.com> that the unit price of the battery is approximately $s_{\text{bat}}^{\text{unit}} = 100.000 \left[\frac{\text{€}}{\text{MWh}} \right]$. The computation of the consumption cost yields the results reported in Table 14.

\mathcal{T}_{bat}	6	12	24
η^{save}	0.11	0.15	0.21
T_a	4.45	6.73	9.93

Table 7: Amortization time T_a (in year) for different battery duration.

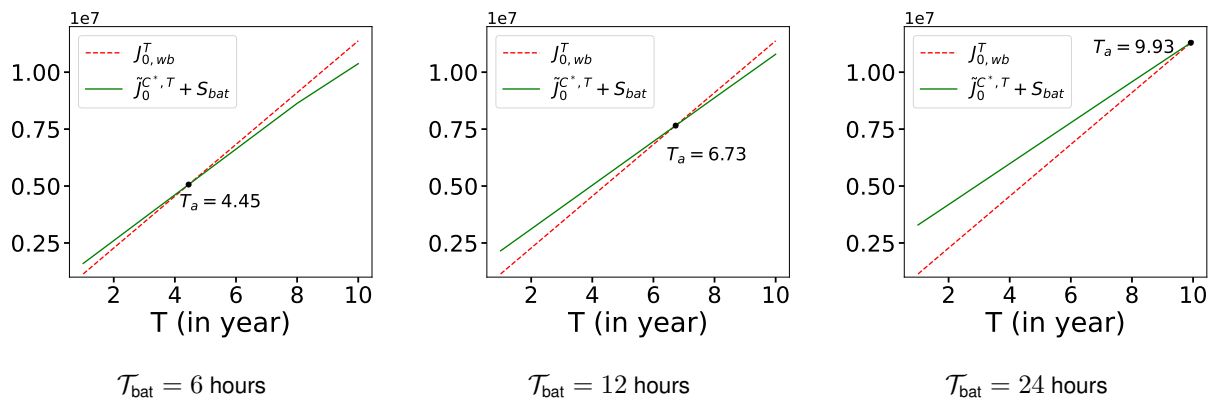


Figure 9: Amortization time T_a for different battery durations \mathcal{T}_{bat} .

From Table 7, we observe that the amortization time T_a naturally increases with the size of the battery, since larger storage capacities require higher investment costs. Further details on the computation of these values are provided in Table 14. Figure 9 illustrates the evolution of the cost without battery, $J_{0,wb}^T(S_0)$, and the optimized cost with battery, $\tilde{J}_0^{C^*,T}(y_0, S_0) + S_{\text{bat}}$, over the time horizon.

A key insight is that the intersection point of these two curves where Equation 44 is satisfied provides a precise estimate of the amortization time. For example, for a battery with a duration of $\mathcal{T}_{\text{bat}} = 24$ hours, our results show that electricity consumption costs can be reduced by up to 21% compared to a strategy without storage. Accumulating these savings over time, the initial investment is recovered after approximately $T_a = 9.93$ years. This outcome is highly relevant from an industrial and economic standpoint: a high quality battery typically has a lifespan of about 15 years. However, after the amortization point is reached, the system benefits from roughly seven additional years of net financial gain. In other words, integrating such a battery into the consumption strategy provides not only technical flexibility but also a clear and quantifiable long term economic advantage.

7 Conclusion

In this work, we investigated the management of stationary battery storage under uncertainty in future electricity spot prices. To this end, we modelled the spot price using a two factor mean reverting model with seasonality, calibrated to real

world data. Two battery models were developed: a simplified formulation based on state of charge constraints and a more realistic model incorporating voltage constraints. These specifications allowed us to formulate the cost minimization problem as a stochastic optimal control problem with state constraints and C-rate control, solved using dynamic programming combined with the LSMC method. Numerical analysis revealed that with a state of charge discretisation of $N_y = 16$ points and a time step of $\Delta t = 0.125$, the model accurately approximated electricity consumption costs with 1% tolerance error, offering a reasonable trade-off between numerical accuracy and computational efficiency. The resulting optimal policies highlighted clear differences between the two battery models: the state of charge model exhibited bang-bang behaviour, while the voltage based model reduced C-rate gradually when approaching full capacity. Although the state of charge model produced lower cost estimates, the voltage based model was retained for analysis due to its higher physical realism. Based on this model, we studied potential cost savings and amortization times for different battery durations. Over a one year horizon time, a battery with $\mathcal{T}_{\text{bat}} = 6$ hours yielded approximately 11% savings compared to a no-storage strategy. This saving increased to 15% for $\mathcal{T}_{\text{bat}} = 12$ hours and became even more substantial for $\mathcal{T}_{\text{bat}} = 24$ hours. We further observed that increases in operational constants or internal resistance reduced battery usage, as they accounted for higher costs. We also approximated the Amortization time, and we obtained approximately $T_a = 4.45$ years for $\mathcal{T}_{\text{bat}} = 6$ hours and $T_a = 6.73$ years for $\mathcal{T}_{\text{bat}} = 12$ hours. Therefore, integrating a stationary battery storage device into the electricity consumption strategy offers not only technical flexibility but also long-term economic benefits. This combination of operational adaptability and financial gain highlights the central role of battery storage in modern energy management.

However, it is important to note that, the results presented here are based on the simplifying assumption that the battery does not degrade over time. In future research, this assumption will be relaxed to include degradation effects. Incorporating ageing into the model will allow us to assess how it influences both the optimal consumption strategy and the payback period, providing a more realistic and comprehensive evaluation for long term operational planning.

Physical Parameters		
Parameters	Description	Unit
Q	Capacity of the Battery	[Ah]
Q_0^{\max}	Initial maximum capacity of the Battery	[Ah]
y^{SOC}	State of charge of the battery	[-]
y_{\min}^{SOC}	Minimum state of charge of the battery	[-]
y_{\max}^{SOC}	Maximum state of charge of the battery	[-]
I	Current	[A]
C	Rate of charge and discharge of the battery	[-]
C_{\min}	Minimum C-rate	[-]
C_{\max}	Maximum C-rate	[-]
T_{bat}	Battery duration	[h]
P_{bat}	Battery power	[W]
P_{dmd}	Power demand	[W]
$E_{\text{dmd}}^{\text{T}_{\text{bat}}}$	Energy demand	[Wh]
V	Voltage of the battery	[V]
V^{OCV}	Open-circuit voltage of a cell	[V]
V_{nom}	Nominal voltage of the battery	[V]
V_{max}	Maximum voltage of the battery	[V]
V_{min}	Minimum voltage of the battery	[V]
\tilde{R}	Internal resistance of the battery	[Ω]
P_c	Operational constant	[1/Mwh]
$s_{\text{bat}}^{\text{unit}}$	Unit price of the battery	[€/Mwh]

Table 8: Physical parameters and values

Electricity spot price parameters and Values		
Parameters	Description	Unit
λ_1, λ_2	speed of mean reversion	[1/h]
μ	long term mean	[€/Mwh]
σ	volatility of the deseasonalized spot price	[€/Mwh \sqrt{h}]
$d_{\text{day}^{(i)}}, d^{(h)}$	daily and hourly dummy variables	[-]
$A_0, A_1, A_2, A_3, C_{\text{day}^{(i)}}^{(h)}$	parameters of Λ	[€/Mwh]

Table 9: Electricity spot price parameters and values

Numerical parameters		
Parameters	Description	Value
Δt	Time step	0.125
N_y	Number of SOC grid points	16
M_{train}	Number of training samples	10^3
M_{test}	Number of testing samples	$2 \cdot 10^4$
r	Discount rate	0
d_y	Dimension of battery state vector	1
d_s	Dimension of electricity price state vector	1

Table 10: Numerical parameters

A Electricity spot price model

A.1 Parameter estimation of the electricity spot price model

The parameters estimation of our two-factor electricity spot price model is done in several steps:

Step 1 (Data extraction): We recall that we consider German and Austrian daily electricity spot price data from the *ENTSO-E Transparency Platform* (<https://newtransparency.entsoe.eu/market/energyPrices>) covering the period from January 1, 2023, to January 1, 2024. For each of the 365 days in this sample, we observe a 24-dimensional vector of hourly prices yielding a total of 8,758 data points. We define the price for hour h , where $h \in \{0, \dots, 23\}$, as the electricity price delivered during the time interval $[h, h + 1)$. Our analysis encompasses the entire dataset, including weekends.

Step 2 (Estimation of the seasonality parameters): To calibrate the parameters of the seasonality function Λ , the first step involves estimating the parameters of the linear trend along with the yearly seasonal component (presented in Table 11) using non-linear least squares regression. The estimated general trend is then subtracted from each of the 24 time series.

Parameter	A_0	A_1	A_2	A_3
Value	148.47	-0.01	30.41	11902.35

Table 11: Calibrated parameter values for the linear trend and the yearly seasonal component.

Next, we calibrate the parameters for the weekly seasonal effects. To do this, we follow the approach of [Ver16]. Specifically, we compute trimmed means of the de-trended data by removing 1% of each side of observations (i.e., a total of 2% of the data). The resulting parameter estimates are presented in Table 12.

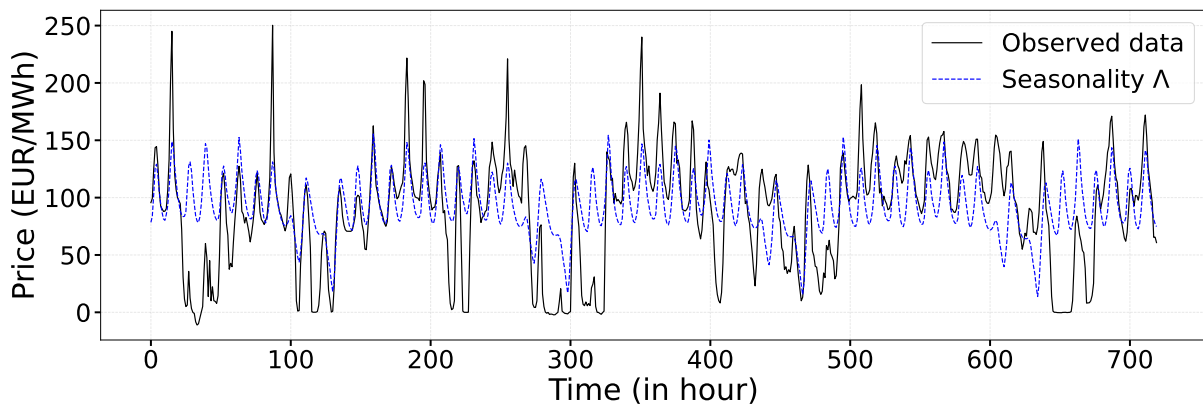


Figure 10: Seasonality function Λ and observed data for October 2023.

In Figure 10, we illustrate the seasonality function Λ based on the calibrated parameters, focusing on the period from October 1 to October 31, 2023. In the next step we use the deseasonalized data to calibrate the stochastic component of the two-factor model.

Step 3 (Extraction of spikes and Brownian-driven component in the deseasonalized spot price): Secondly, the spikes component in the deseasonalized spot price series is identified and separated from the base component. Among the two methods developed in [MBT08], namely hard thresholding and the adapted Potts filter, we choose to implement the hard thresholding method. Given a fixed number M of spikes to be removed from the deseasonalized data, we first estimate from the autocorrelation function the mean-reversion coefficients $\lambda_1 = 0.1$ and $\lambda_2 = 0.148$. Thereafter, the maximum likelihood estimators (MLE) for the spike parameters (spike sizes and times) (α_i, τ_i) , $i = 1, \dots, M$, are

Hour	Monday	Tuesday	Wednesday	Thursday	Friday	Saturday	Sunday
0	-16.724	-9.316	-12.133	-11.221	-17.736	-24.586	-21.579
1	-11.357	-5.116	-6.477	-6.922	-17.116	-24.257	-14.267
2	7.744	14.932	9.926	9.778	-15.190	-24.427	5.832
3	30.662	34.208	28.526	25.109	-11.634	-23.885	26.596
4	33.755	37.259	33.315	29.676	-9.296	-25.278	30.970
5	23.444	28.531	26.439	24.427	-11.538	-29.787	21.595
6	8.188	11.705	13.484	13.221	-19.916	-39.312	5.273
7	-1.807	-0.817	5.394	3.814	-30.087	-48.347	-4.968
8	-9.135	-11.561	0.013	-5.722	-37.629	-55.561	-12.965
9	-14.715	-15.912	-6.740	-13.499	-46.367	-67.070	-19.026
10	-15.865	-17.004	-7.553	-16.322	-49.919	-75.638	-19.728
11	-10.728	-12.268	-2.460	-12.876	-40.650	-64.867	-14.873
12	-3.034	-1.109	6.172	-4.401	-27.072	-40.980	-6.709
13	12.262	16.271	18.846	7.978	-7.546	-16.327	7.074
14	33.193	35.627	39.355	25.736	13.094	7.547	31.793
15	54.296	52.671	58.637	37.536	25.171	22.868	59.586
16	48.688	48.676	47.227	32.054	21.903	25.094	49.838
17	32.383	32.598	29.739	17.963	13.763	18.076	28.223
18	20.985	18.000	18.573	7.311	5.710	10.700	14.181
19	8.004	7.603	8.424	-1.136	-1.191	3.088	4.068
20	1.975	-0.355	0.592	-6.743	-9.208	-4.770	-5.194
21	-4.936	-6.351	-5.828	-11.159	-14.996	-12.798	-10.947
22	-7.916	-10.187	-9.443	-14.913	-20.027	-18.404	-14.329
23	-9.638	-12.634	-11.448	-17.316	-22.863	-20.930	-16.579

Table 12: Trimmed means for the data after removing the trend. The trimmed means exclude 2% of the data, i.e., 1% on each side.

obtained via least squares estimation. To optimally choose M , we fix a target noise level of $\varepsilon = 2\%$, i.e. 2% of all returns are to be removed. This yields a target standard deviation of $\sigma^* = 36.77$ (the standard deviation computed using all available data is 42.38). To achieve this target noise level, the extraction of $M = 188$ Jumps is needed.

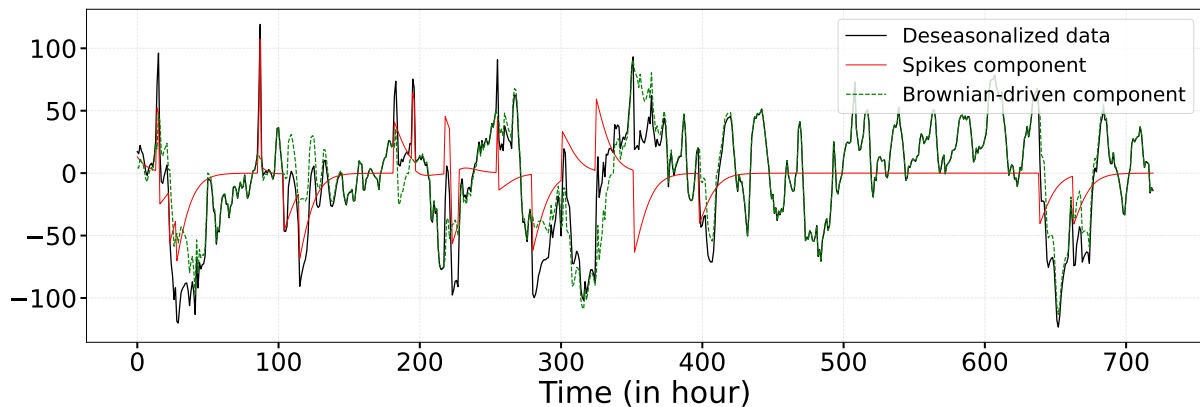


Figure 11: Decomposition of the deseasonalized spot price into a Brownian-driven component and a spike component using hard thresholding on deseasonalized data (visualization for October 2023).

Step 4 (Estimation of base component): After the spike component is removed, the increments of the base component (deseasonalized data without spikes) exhibit near-Gaussian behaviour. Indeed, in the case of the *ENTSO-E Transparency Platform* electricity price data, the increments of the base component have a skewness of -0.7245 (up from -1.0119 for the initial deseasonalized data including spikes) and an excess kurtosis of 0.81 (down from 8.32). Based on our analysis, the base component closely approximates a Gaussian distribution, making it suitable for modelling with an AR(1) process featuring Gaussian increments. The parameters of the first Ornstein-Uhlenbeck process are calibrated through maximum

likelihood, yielding

$$\lambda_1 = 0.0389, \quad \mu = 0.9972, \quad \sigma = 10.1653. \quad (45)$$

Step 5 (Estimation of the spike component): Concerning the spike component, the goal is to estimate both the intensity of jumps and the distribution of the spike amplitudes. The spike occurrence dates, obtained from the separation step, allow us to construct a maximum likelihood estimator for the spike intensity. Specifically, when N is a time inhomogeneous Poisson process with time dependent intensity $\lambda(t) > 0$, the driving process for the spike component is modelled as

$$L_2(t) = \sum_{i=1}^{N(t)} B_i Z_i, \quad (46)$$

where, Z_1, Z_2, Z_3, \dots are i.i.d. random variables following a Pareto distribution with parameters (z_0, α) and B_1, B_2, B_3, \dots are i.i.d. Bernoulli random variables taking values in $\{-1, +1\}$ with success probability p_2 . We choose a Pareto distribution because the spike amplitudes are bounded from below by some threshold $z_0 > 0$ and hence we need a distribution supported on the interval $[z_0, +\infty)$; also the number of data points available for estimation is limited (188 spikes). The time dependent intensity $\lambda(t)$ is defined as

$$\lambda(\theta_1, \theta_2, t) = \theta_1 f(t)^{\theta_2} \quad \text{with} \quad f(t) = \frac{1}{1 + \left| \sin\left(\frac{\pi(t-t_0)}{365 \cdot 24}\right) + 0.01 \right|^2} - \frac{1}{2}. \quad (47)$$

It produces a seasonal intensity that peaks at $t = t_0$ and exhibits symmetric decay across the whole time interval. Using maximum likelihood, we estimate $\theta_1 = 0.0451$ and $\theta_2 = 0.882$ with a maximum ($t_0 = 255 \cdot 24$) between August and September. The parameters of the Pareto distribution (the smallest spike amplitude z_0 and the decay rate α), as well as the Bernoulli probability p_2 , are estimated by maximum likelihood from the extracted jump data. We obtain

$$\lambda_2 = 0.168, \quad \alpha = 2.44, \quad z_0 = 43.02, \quad p_2 = 0.5051. \quad (48)$$

This model specification enables the simulation of price trajectories. As illustrated in Figure 12, the model effectively replicates the observed behaviour of the spot price series.

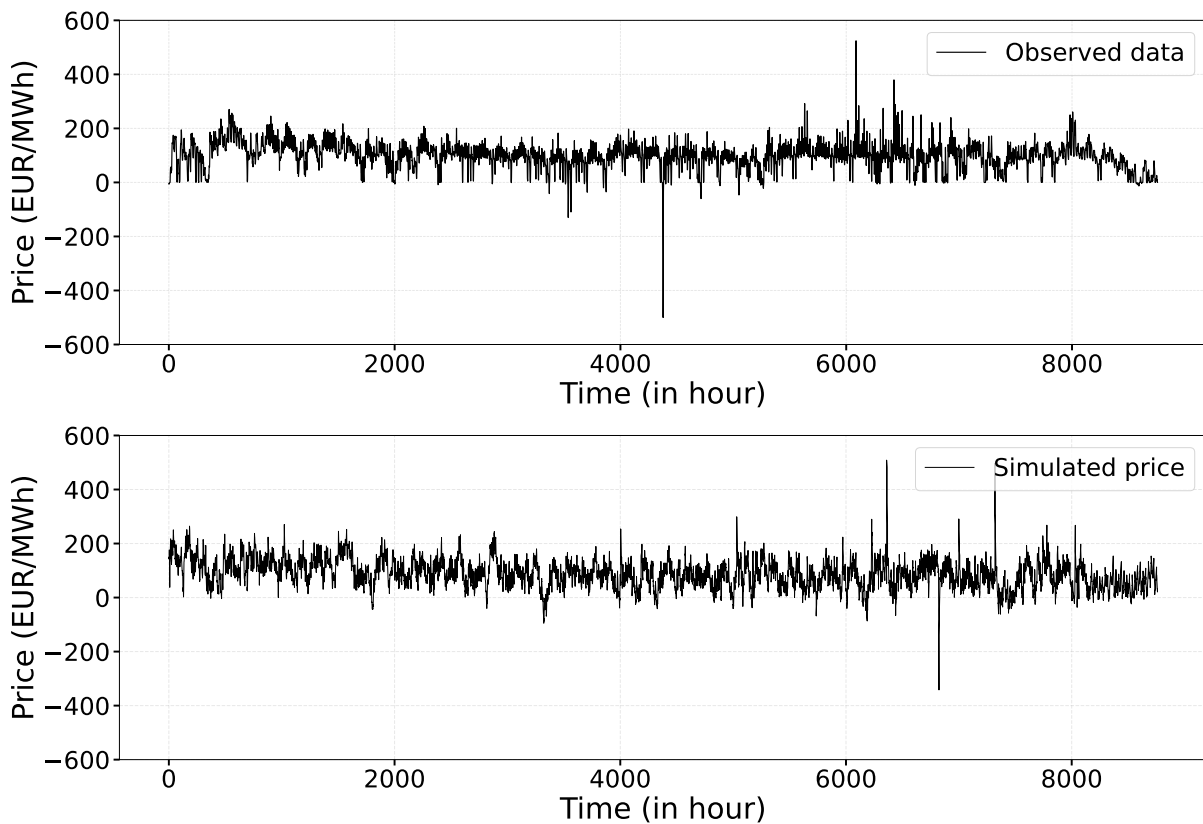


Figure 12: Real German and Austrian daily electricity spot price data and a sample spot price trajectory simulated with the calibrated parameters of our two-factor model.

B Internal resistance

In order to deeply study the sensitivity of $\tilde{J}_0^{C^*}(y_0, S_0)$ with respect to the internal resistance of the battery. Due to computational constraints, we present in Table 13 the consumption cost as a function of R for different values, considering a time horizon of $T = 24 \cdot 30$ hours. This table focuses on a representative set of resistance values.

R	0	0.2	0.4	0.6	0.8	1.0	1.2
$\tilde{J}_0^{C^*}$	92227.79	93345.88	93522.80	93676.56	93819.16	93956.66	94107.97
MC error	123.396	124.794	125.015	125.067	125.104	125.098	125.051
R	1.4	1.6	1.8	2.0	2.2	2.4	2.6
$\tilde{J}_0^{C^*}$	94258.54	94348.87	94456.09	94692.81	94757.70	94770.27	94770.27
MC error	124.911	125.149	125.096	124.837	125.142	124.708	124.708

Table 13: Consumption cost $\tilde{J}_0^{C^*}(y_0, S_0)$ for different internal resistance values R for $T = 24 \cdot 30$ hours. We used 10^3 training samples, $2 \cdot 10^4$ testing samples, $N_y = 16$, initial SOC of the battery $y_0^{\text{SOC}} = 0$, $\Delta t = 0.125$ hour and $\mathcal{T}_{\text{bat}} = 24$.

C Amortization time

In the original spot price model, the presence of a negative linear trend implies that electricity prices decrease over the years. As the time horizon increases, this trend eventually pushes the spot price into negative values. When this happens, estimating an amortization horizon becomes conceptually unreliable, since the economic environment simulated is no longer representative of realistic market conditions. To ensure that the amortization analysis remains meaningful, we therefore set the long term trend parameter to zero ($A_1 = 0$). This assumption removes the artificial long run drift while preserving the realistic intra day and seasonal fluctuations of the price process. In other words, the annual price structure is kept stable across years, which is consistent with many empirical electricity price models used for long-term planning.

In addition, removing the linear trend does not affect the qualitative behaviour of the optimal charging policy, and the relative performance between scenarios remain structurally unchanged. The assumption simply ensures that the long-term cost comparison and the resulting amortization period are evaluated under a stable and economically plausible price regime. Thus, the reported results in Table 14 remain robust and fully interpretable.

T	$J_{wb,0}^T$	$\mathcal{T}_{\text{bat}} = 6$ hours		$\mathcal{T}_{\text{bat}} = 12$ hours		$\mathcal{T}_{\text{bat}} = 12$ hours	
		$\tilde{J}_0^{C^*,T}$	η^{save}	$\tilde{J}_0^{C^*,T}$	η^{save}	$\tilde{J}_0^{C^*,T}$	η^{save}
24 · 365	1139293.50±	1001096.95±	0.121	954967.14 ±	0.161	890571.06 ±	0.218
	439.34	455.60		479.54		525.76	
24 · 365 · 2	2277828.31±	2003993.91±	0.120	1912784.20±	0.160	1785083.55±	0.216
	622.10	648.33		682.29		747.51	
24 · 365 · 4	4553601.76±	4013156.84±	0.118	3833926.66±	0.157	3581084.84±	0.213
	886.90	911.26		958.00		1047.13	
24 · 365 · 6	6827406.57±	6022178.77±	0.117	5756255.39±	0.156	5380759.57±	0.211
	1082.58	1117.08		1172.40		1278.96	
24 · 365 · 8	9102121.74±	8030191.87±	0.117	7676777.85±	0.156	7176687.72±	0.211
	1248.50	1291.92		1355.22		1478.42	
24 · 365 · 10	11375914.69±	9773080.49±	0.140	9586273.99±	0.157	8957488.33±	0.212
	1394.26	1424.39		1514.26		1653.91	

Table 14: Total consumption cost for different values of battery duration \mathcal{T}_{bat} and different time period T . We used 10^3 training samples, $2 \cdot 10^4$ testing samples, $N_y = 16$, initial SOC of the battery $y_0^{\text{SOC}} = 0$ and $\Delta t = 1$ hour.

References

- [BJM⁺17] Ines Baccouche, Sabeur Jemali, Bilal Manai, Noshin Omar, and Najoua Essoukri Ben Amara. Improved OCV model of a Li-ion NMC battery for online SOc estimation using the extended Kalman filter. *Energies*, 10(6):764, 2017.
- [BR11] Nicole Bäuerle and Ulrich Rieder. *Markov decision processes with applications to finance*. Springer Science & Business Media, 2011.
- [CMBP⁺25] Javier Cardo-Miota, Hector Beltran, Emilio Pérez, Shafi Khadem, and Mohamed Bahloul. Deep reinforcement learning-based strategy for maximizing returns from renewable energy and energy storage systems in multi-electricity markets. *Applied Energy*, 388:125561, 2025.
- [CT18] Y Chen and M Trifkovic. Optimal scheduling of a microgrid in a volatile electricity market environment: Portfolio optimization approach. *Applied Energy*, 226:703–712, 2018.
- [CWCY25] Jun Cai, Kangli Wang, Adrian David Cheok, and Ying Yan. Optimal configuration for power grid battery energy storage systems based on payload fluctuation guided multi-objective PSO. *Journal of Energy Storage*, 105:114515, 2025.
- [DFG21] Thomas Deschatre, Olivier Féron, and Pierre Gruet. A survey of electricity spot and futures price models for risk management applications. *Energy Economics*, 102:105504, 2021.
- [EGASNH25] Mahmoud El-Ghazaly, Mazen Abdel-Salam, Mohamed Nayel, and Mohamed Hashem. Techno-economic utilization of hybrid optimized gravity-supercapacitor energy-storage system for enriching the stability of grid-connected renewable energy sources. *Journal of Energy Storage*, 107:115002, 2025.
- [ETI25] ETIP SNET. Renewable energy sources to account for 85% of global electricity production by 2050. <https://smart-networks-energy-transition.ec.europa.eu/news/renewable-energy-sources-account-85-global-electricity-production-2050>, 2025. Accessed: 2025-08-21.
- [Eur24] Euro Inox. Real Cost Behind Grid-Scale Battery Storage: 2024 European Market Analysis. <https://www.euro-inox.org/real-cost-behind-grid-scale-battery-storage-2024-european-market-analysis>, 2024. Accessed: 2025-10-18.
- [How60] Ronald A. Howard. *Dynamic Programming and Markov Processes*. MIT Press, Cambridge, MA, USA, 1960.
- [KPS19] Rüdiger Kiesel, Florentina Paraschiv, and Audun Sætherø. On the construction of hourly price forward curves for electricity prices. *Computational Management Science*, 16(1):345–369, 2019.
- [KWZ23] Gaurav Kapoor, Nuttanan Wichitakorn, and Wenjun Zhang. Analyzing and forecasting electricity price using regime-switching models: The case of New Zealand market. *Journal of Forecasting*, 42(8):2011–2026, 2023.
- [MBT08] Thilo Meyer-Brandis and Peter Tankov. Multi-factor jump-diffusion models of electricity prices. *International Journal of Theoretical and Applied Finance*, 11(05):503–528, 2008.
- [MVB⁺20] Kendall Mongird, Vilayanur Viswanathan, Patrick Balducci, Jan Alam, Vanshika Fotedar, Vladimir Koritarov, and Boualem Hadjerioua. An evaluation of energy storage cost and performance characteristics. *Energies*, 13(13):3307, 2020.
- [MZC⁺20] R Machlev, N Zargari, NR Chowdhury, J Belikov, and Y Levron. A review of optimal control methods for energy storage systems-energy trading, energy balancing and electric vehicles. *Journal of Energy Storage*, 32:101787, 2020.
- [NNN25] Thuan Thanh Nguyen, Thang Trung Nguyen, and Hoai Phong Nguyen. Optimal operation of battery energy storage system in microgrid to minimize electricity cost based on model predictive control using coyote algorithm. *Journal of Energy Storage*, 114:115904, 2025.
- [PPW⁺20] Saehong Park, Andrea Pozzi, Michael Whitmeyer, Hector Perez, Won Tae Joe, Davide M Raimondo, and Scott Moura. Reinforcement learning-based fast charging control strategy for Li-ion batteries. In *2020 IEEE Conference on Control Technology and Applications (CCTA)*, pages 100–107. IEEE, 2020.

- [PSK⁺22] Prarthana Pillai, Sneha Sundaresan, Pradeep Kumar, Krishna R Pattipati, and Balakumar Balasingam. Open-circuit voltage models for battery management systems: A review. *Energies*, 15(18):6803, 2022.
- [SDD24] Stephan Schlüter, Abhinav Das, and Matthew Davison. Optimal Control of a Battery Storage On the Energy Market. In *2024 IEEE/IAS Industrial and Commercial Power System Asia (I&CPS Asia)*, pages 102–107. IEEE, 2024.
- [Ver16] Almut ED Veraart. *Modelling the impact of wind power production on electricity prices by regime-switching Lévy semistationary processes*. Springer International Publishing, 2016.
- [VM25] Arjen T Veenstra and Machiel Mulder. Profitability of batteries in day-ahead and intraday electricity markets: Assessment of operation strategies with endogenous prices. *Energy Economics*, page 108608, 2025.
- [WSP14] Caihao Weng, Jing Sun, and Hwei Peng. A unified open-circuit-voltage model of lithium-ion batteries for state-of-charge estimation and state-of-health monitoring. *Journal of power Sources*, 258:228–237, 2014.